applied sciences

MDPI

Review

Thermal Conductivity of Nanofluids: A Review on Prediction Models, Controversies and Challenges

Inês Gonçalves [1,2,†], Reinaldo Souza [2,†], Gonçalo Coutinho [1], João Miranda [3], Ana Moita [1,4], José Eduardo Pereira [1], António Moreira [1] and Rui Lima [2,*]

1 IN+Center for Innovation, Technology and Policy Research, Instituto Superior Técnico, Universidade de Lisboa, Av. RoviscoPais, 1049-001 Lisboa, Portugal; inesmaiag@gmail.com (I.G.); goncalo.coutinho@tecnico.ulisboa.pt (G.C.); anamoita@tecnico.ulisboa.pt (A.M.); sochapereira@tecnico.ulisboa.pt (J.E.P.); aluismoreira@tecnico.ulisboa.pt (A.M.)
2 MEtRICs, Mechanical Engineering Department, University of Minho, Campus de Azurém, 4800-058 Guimarães, Portugal; reisartre@gmail.com
3 CEFT, Faculdade de Engenharia da Universidade do Porto (FEUP), R. Dr. Roberto Frias, 4200-465 Porto, Portugal; jmiranda@fe.up.pt
4 CINAMIL–Military Academy Research Center, Portuguese Military Academy, R. Gomes Freire, 203, 1169-203 Lisboa, Portugal
* Correspondence: rl@dem.uminho.pt
† These authors contributed equally to this work.

Abstract: In recent years, the nanofluids (NFs) have become the main candidates for improving or even replacing traditional heat transfer fluids. The possibility of NFs to be used in various technological applications, from renewable energies to nanomedicine, has made NFs and their thermal conductivity one of the most studied topics nowadays. Hence, this review presents an overview of the most important advances and controversial results related to the NFs thermal conductivity. The different techniques used to measure the thermal conductivity of NFs are discussed. Moreover, the fundamental parameters that affect the NFs thermal conductivity are analyzed, and possible improvements are addressed, such as the increase of long-term stability of the nanoparticles (NPs).The most representative prediction classical models based on fluid mechanics, thermodynamics, and experimental fittings are presented. Also, the recent statistical machine learning-based prediction models are comprehensively addressed, and the comparison with the classical empirical ones is made, whenever possible.

Keywords: nanofluids; nanoparticles; thermal conductivity; heat transfer; machine learning

Citation: Gonçalves, I.; Souza, R.; Coutinho, G.; Miranda, J.; Moita, A.; Pereira, J.E.; Moreira, A.; Lima, R. Thermal Conductivity of Nanofluids: A Review on Prediction Models, Controversies and Challenges. *Appl. Sci.* **2021**, *11*, 2525. https://doi.org/10.3390/app11062525

Academic Editor: Yulong Ding

Received: 19 February 2021
Accepted: 6 March 2021
Published: 11 March 2021

1. Introduction

Technological development in the past decades led to the increase in demand for novel cooling fluids able to surpass the conventional ones—air and water—to improve the lifespan of the electronic components [1]. One type of fluid that has been increasingly investigated is nanofluid (NF), as seen in Figure 1. Introduced in 1995 by Stephen Choi, nanofluids consist of a colloidal dispersion of nanoparticles (NPs) with 1–100 nm of dimension in a base fluid (BF) [2,3].

The NPs usually used in the NFs are oxides, metals, nitrides, and non-metals like carbon nanotubes and graphene, while the BF are often water, ethylene glycol, oils, and polymer solutions [4].

NFs contribute to the improvement of heat transfer processes, and to reduce and optimize thermal systems [5].Different properties, such as wettability and thermal conductivity, can be adjusted by altering the NPs concentration, making nanofluids suitable for a wide range of applications. Local concentration can be controlled using magnetic NPs under the action of an applied magnetic field [6]. Nevertheless, preparation and use of NFs still have some limitations. Sedimentation and aggregation of the particles are difficult to control and

may accelerate corrosion of the components and increase the dynamic viscosity of the NFs. Also, the synthesis of nanomaterials is still an expensive process [5].On top of that, there is no general consensus regarding the exact concentration and type of particle required for the NFs best performance. In spite of these difficulties, new and more competitive preparation techniques have been developed. For example, titanium dioxide NFs can be obtained nowadays by the Vapor Deposition Technique (VDT) [7].

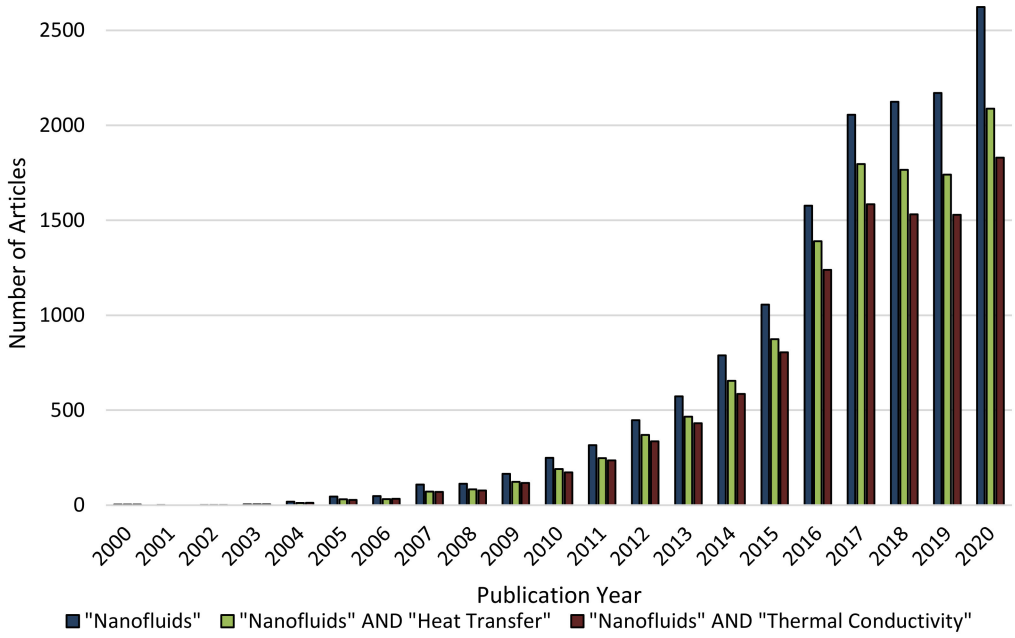

Figure 1. Number of scientific journal articles presented in the Science Direct database published between January of2000 and September of 2020.(Search date: 10.09.2020) (Please read the data availability statement).

Due to the previously mentioned advantages, NFs have been applied to a wide variety of fields [6–9]. For instance, some NFs were used to cool electronic parts such as CPUs [10] and transformers [11], motor engines [12] and nuclear reactors [13]. In space technologies, they were tested to improve cooling mechanisms, and also as fuel [14] and for machining and grinding techniques as lubricant and cutting fluid [15]. The thermal properties of NFs were also very useful to improve the heat transport and, consequently, the thermal efficiency of systems like heat pipes [16], thermosiphons [17], heat exchangers, and chillers [6,8], and solar panels and collectors [17]. Recently, there has been a growing interest in the use of NFs in nanomedicine. On this field, the magnetic NPs can be used not only to improve the potential of diagnostic techniques but also in hyperthermia treatments or as drug carriers [18–21].Also, the use of NFs to study the heat transfer mechanisms in cavities, like the free natural convection, has grown tremendously [22].

One of the most relevant properties of NFs is the thermal conductivity. The thermal conductivity of NFs is influenced by shape, size, concentration and surface resistance of the NPs and by the viscosity, pH, temperature, and other characteristics of the base fluid [23]. Several theoretical models and experimental methods were developed to measure this property. The most common measuring methods are the transient hot-wire method followed by the 3ω method, the steady-state parallel plate method and the temperature oscillation method. Despite the growing number of studies, there are still disparities between data generated by the theoretical models and experimental measurements as well as between measurements derived from the same method (reproducibility of results) [3].

In this work, the main experimental methods used by researchers to measure the thermal conductivity of nanofluids will be presented. The study will discuss the parameters that may be interfering with the accuracy of the results like the aforementioned factors, and

also the relevant role of concentration, temperature, viscosity, heat capacity, and surface tension of the resulting nanofluid.

2. Thermal Conductivity Measurements Overview

The current methods developed for thermal conductivity measurements are static methods and can be divided in Steady State Methods and Transient State Methods. The Steady State Methods comprise the parallel plane and coaxial cylinders methods, while the Transient State Methods include the transient hot wire, the transient plane source theory, the temperature oscillation method, the laser flash method and the 3ω method [24]. A brief description of the techniques will be presented in the following subsections. Figure 2 shows the steady and transient state methods often used to measure the thermal conductivity of the NFs.

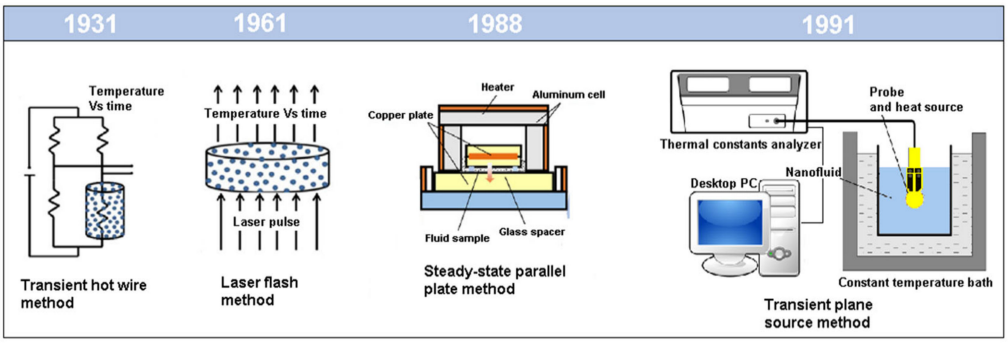

Figure 2. Schematic diagram of steady and transient state methods to measure the thermal conductivity of nanofluids (NFs) (Adapted from [5]).

2.1. Transient Hot Wire Method

In this technique, a very thin metal wire, usually of platinum or tantalum, is used as both heat source and sensor. The wire is submerged on the NF, and a certain voltage is applied through the wire, heating it. The heat will then be transferred to the surrounding liquid at a rate depending on the thermal conductivity of the liquid. The resistance variations measured in the wire can be correlated with the temperature variations and, therefore, the thermal conductivity is calculated. Systematic errors that might affect the measurements, such as errors resulting from natural convection, can be corrected experimentally [5,24].

2.2. Transient Plane Source Theory

A fast and sensitive technique with similar principle as the transient hot wire consists of replacing the wire by a hot disk. Similarly, to obtain the temperature and thus calculate the thermal conductivity, the time variation of the electrical resistance is recorded. Like in the case of the Transient Hot Wire Method, convection currents in the fluid might affect the measurements [5,24].

2.3. Temperature Oscillation

The fluid is placed in a cylinder with an oscillating temperature being applied at both ends. The amplitude and phase of the temperature oscillation in the middle of the cylinder are registered. To avoid interferences from the convection phenomena, the amplitude of the applied oscillation should be as small as possible [24,25].

2.4. 3ω Method

The metal heater in the fluid is heated by a sinusoidal electric current with an angular frequency of ω, leading to temperature oscillations in the fluid with a certain frequency. Then, the frequency is correlated with the thermal conductivity of the NF. This technique requires small amounts of fluid and is more suitable for non-spherical particles, accord-

ing [5] are more suitable for nanotubes, nanowires, and nanofins. On the other hand, it takes more time than the other techniques to obtain the results [5,24].

2.5. Laser Flash Method

The bottom of the fluid is heated with a laser and the temperature on the top of the fluid is measured with a thermometer. The temperature increase can then be correlated with the thermal conductivity. The effects of radiation and convection are minimized by the short time (in the order of nanoseconds) needed to heat the sample [5].

2.6. Parallel Plate

The sample is placed between two round parallel plates made of copper with incorporated thermocouples. One of the plates is heated, and the temperature difference between the plates will be correlated with the thermal conductivity. To obtain a homogeneous thickness and to minimize convection due to gravity, both plates can be leveled while the sample is being loaded [5,24].

2.7. Coaxial Cylinders

The thermal conductivity of nanofluid can be calculated in the gap by using the Fourier equation in cylindrical co-ordinates. The natural convection is reduced by using very small temperature gradients [24].

3. Parameters That Affect Thermal Conductivity

The thermal conductivity of the NFs can be affected by several factors, since many preparation parameters can vary widely, as presented in the Figure 3. From the characteristics of the NPs to their stability in the fluid, as well as other properties of the suspension, all those factors contribute, directly or indirectly, to induce variations in the thermal conductivity. A brief description of the effect of each factor in the thermal conductivity will be presented in the following sub-sections.

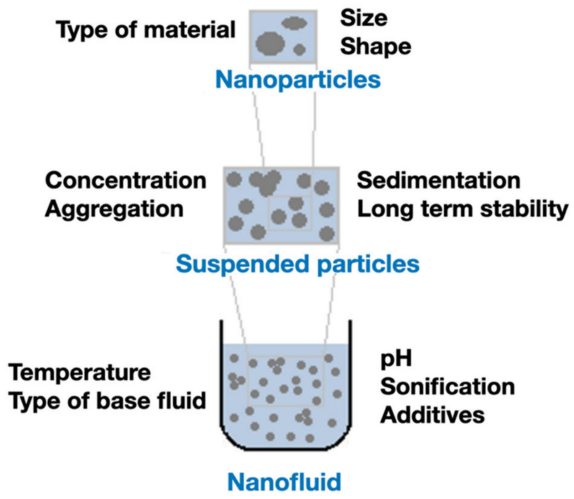

Figure 3. Different properties that affect the thermal conductivity of NFs (Adapted from [5]).

3.1. Nanoparticles (NPs)

3.1.1. Type

Different types of NPs have been tested, such as metals, metal oxides, ceramics, and carbon nanotubes. Some reports indicate that the thermal conductivity of the NPs is less relevant to increase the NFs heat transfer rates, while others suggest that NPs with higher values of thermal conductivity may increase the heat transfer in the NFs [26]. For instance, Wang et al. [27] compared the thermal conductivity of water-based nanofluids with copper and alumina NPs. The greater enhancement of the thermal conductivity in the copper

nanofluid was attributed to the higher thermal conductivity of copper. On the other hand, Yoo et al. [28] observed a greater enhancement in thermal conductivity using a water-based nanofluid with TiO_2NPs than when using Al_2O_3NPs, despite the lower values of the thermal conductivity of the TiO_2NPs.

3.1.2. Size

The influence of the size of the NPs is still controversial among the scientific community. Ambreen and Kim [29] believed that the reduction of the size of NPs increases the effective surface area, thickens the interfacial layering, and enhances the Brownian motion. For these reasons, the thermal conductivity of the nanofluids increases with the reduction of the particle diameter. Xu et al. [30] measured the thermal conductivity of water-based NF with Al_2O_3NPs of different sizes and registered a reduction of the thermal conductivity with increasing sizes. Anoop et al. [31] also compared NFs with alumina NPs of 45 and 150 nm of dimensions. The higher enhancement was reported for the smaller particles. Although most of the results presented in the available literature agree with that proposition, a few others suggest opposite conclusions. Jang and Choi [32] registered an increase of the thermal conductivity with increasing particle size for different types of NPs. Timofeeva et al. [33] compared water-based NFs with four different sizes of SiC NPs and obtained higher values of thermal conductivity with the bigger particles. It should also be noted that for nearly micrometer-sized particles, the Brownian motion is not present, and the thermal conductivity remains unchanged. For a small range of particle size, some authors reported a linear increase of conductivity with increasing particle size due to the reduced interfacial thermal resistance of the larger particles [5,26].

3.1.3. Shape

Different shapes of NPs were tested in theoretical and experimental studies with NFs: spherical, cylindrical, rod, banana-shaped, nearly rectangular, brick, platelet, and blade shapes. The results obtained indicate that particles with larger aspect ratios contribute to the enhancement of the thermal conductivity, since thermal penetration increases and the adverse effects of interfacial thermal resistance on heat transfer are reduced. On the other hand, when the particles have a small sphericity factor, the thermal conductivity is not enhanced [5,26]. Murshed et al. [34] observed a greater increase in the thermal conductivity values of water-based TiO_2 NFs when using rod-shape NPs than when using spherical NPs. Jeong et al. [35] obtained similar results when comparing spherical and nearly rectangular-shaped ZnO NPs. Timofeeva et al. [36] compared NFs with four different shapes of Al_2O_3NPs and concluded that the NF with higher thermal conductivity value was the one with cylindrical NPs, followed by the one with brick shape NPs. In addition, the NFs with blade shape and platelet shape particles presented similar values and were also the lower ones among the testing group. Glory et al. [37] investigated the increase of the thermal conductivity using Multi-Walled Carbon Nanotubes (MWCNT)of different lengths, obtaining greater values for the NFs with the longest nanotubes.

3.2. Suspension

3.2.1. Base Fluids

Most studies agree that the base fluids with greater thermal conductivity correspond to NFs with smaller thermal conductivity increases. The reports also suggest that the affinity of the fluid to the NPs has an important role in the thermal conductivity enhancements [26]. For instance, Gowda et al. [38], Chen et al. [39], and Hwang et al. [40] reported higher thermal conductivity values for ethylene glycol-based NFs than water-based NFs, using alumina, MWCNTs, and CuO NPs, respectively.

3.2.2. Concentration

The increase of the particle concentration enhances the thermal conductivity due to the greater interfacial area between the base fluid and the NPs and increasing agglomer-

ation [41,42]. Rostamian et al. [43] and Xuan et al. [44] reported an increase in thermal conductivity by increasing the nanoparticle concentration. Jana et al. [45] also observed a linear relation between concentration and thermal conductivity using water-based copper NFs. Lee et al. [46], using NPs of Al_2O_3 and CuO, measured experimentally the thermal conductivity of the NFs at low volume fraction range (lower than 0.05%) and found that the thermal conductivity ratios increase almost linearly with volume fraction, but with different rates of increase for each group of NPs tested. However, some reports noted a reduction of the thermal conductivity for high concentration values. The stability of the NF is likely to play a major role in the determination of the ideal concentration [5,26].

3.2.3. Agglomeration

The agglomeration of particles contributes to the enhancement of the thermal conductivity by providing extra conduction paths on the NFs. For fluids with smaller particles, the aggregation is more prone to occur. The way the aggregation occurs in NFs with greater volume fractions depends on the shape of the particles. In the studies performed by Hong et al. [47], an increase of thermal conductivity was observed with an increase of the aggregation of the particles in a water-based alumina NF. On the other hand, large agglomerates of particles can lead to sedimentation of the particles and reduction of the thermal conductivity. Jana et al. [45] noted a decrease of thermal conductivity with increase sedimentation time in water-based copper and carbon nanotube NFs. It is possible to locally control the aggregation in NFs with magnetic NPs by means of a magnetic field. The aggregation is also reversible by applying different magnetic fields in different directions [5,26,48]. Li et al. [49] reported an enhancement in the thermal conductivity of an NF with iron particles when applying a magnetic field. Also, Nasiri et al. [50] observed a reduction of the thermal conductivity of a water-based carbon nanotube NF due to the aggregation of the NPs.

3.3. Nanofluids

3.3.1. Preparation Methods

Two methods of preparing nanofluids are commonly used by the scientific community, the one-step, and two-step method. The one-step method involves the production and dispersion of the NPs in the BF at the same time. For this reason, the process reduces the NPs agglomeration and increases stability in the NFs [3]. In contrast, the high cost and level of impurities on the NFs, according to Devendiran et al. [51], are the main disadvantages of this process. In the two-step method, first, the NPs are obtained and then added to the BF. This simplifies the manufacturing process while reducing its cost. However, maintaining the stability of the NFs is one of the challenges of this method. Some alternatives to solve the problem include the use of ultrasonic treatment, altering the pH of the suspension, adding surface activators or dispersants or a mixture of both [51,52].

The high production cost of the nanofluids has been another limitation, which may require a more demanding maintenance of a cooling system and, consequently, raise the operating costs. In addition, the preparation of NFs on a larger scale requires further reduction of its costs since the most cost-effective techniques are the ones considered for commercialization purposes. One way to reduce these costs is by recycling and recover NPs from industrial wastes.

3.3.2. Temperature

Some reports indicate that the thermal conductivity is enhanced with the temperature increase, while others reported a reduction of the thermal conductivity with the same effect. Few others stated that no changes were observed with temperature variations. For instance, Chon et al. [53] and Mintsa et al. [54] registered a dependent behavior between the thermal conductivity of the NFs and temperature, while Shalkevich et al. [55] reported an independent behavior. Duangthongsuk et al. [56], on the other hand, observed a decrease of the thermal conductivity with increasing temperature in a water-based TiO_2 NFs. The

enhancement of the thermal conductivity with increasing temperature is thought to be caused by the improvement of the Brownian motion and the reduction of the surface energy of the particles. On the contrary, a reduction of the thermal conductivity with increasing temperature was reported for NFs with non-spherical particles, which might indicate that the aspect ratio of the particle has a relevant influence [5,26].

3.3.3. pH

The pH of the NFs affects the aggregation degree of the NPs and, consequently, the thermal conductivity. The isoelectric point of the value of pH occurs when the amount of positive and negative ions is the same. Some studies reported an increasing enhancement of the thermal conductivity with increasing pH until the isoelectric point, which is then followed by a decrease. This was attributed to the increase of electrical charge on the surface of the NPs, leading to greater electrostatic repulsion [5,26]. Krishnakumar et al. [57] and Li et al. [58] reported an increase in thermal conductivity with pH of ethanol-based alumina NFs until a maximum value with pH value near 6.0, which is then followed by a decrease with increasing pH. Wang et al. [59] registered similar results with water-based copper and alumina NF, being the maximum thermal conductivity value obtained when the isoelectric point was reached. Other studies showed lower values of thermal conductivity in the isoelectric point, i.e., the repulsive forces among particles are zero, making particles aggregate under this pH value [60]. The experimental work developed by [61] also shown that the pH influences the zeta potential, particle size distribution, rheology, viscosity, and stability, and all these factors affect the thermal conductivity of the NFs containing ZrO_2 and TiO_2 NPs.

3.3.4. Additives, Surfactants and Solvents

The incorporation of additives on the NFs can help to improve the stability of the fluid over time. Wang et al. [27] and Zhu et al. [62] identified the optimal concentration of the surfactant SDBS (Sodium dodecylbenzenesulfonate) to increase the thermal conductivity of water-based copper and alumina NFs. Eastman et al. [63] improved the thermal conductivity of ethylene glycol-based copper NFs by adding thioglycolic acid. High concentrations of additives can lead to negative effects on the NFs, such as flocculation. When adding reduced amounts of additive little or no effect on the thermal conductivity was reported [13,26]. The experimental work developed by [64] demonstrated the impact on the alignment and dispersion of the NPS and on the thermal conductivity of the NFs that the surfactants and solvents may have. In this study, the authors measured the thermal conductivity of Fe_2O_3 and CuO NPs dispersing in water, ethylene glycol, and water with SDBS as a surfactant.

3.3.5. Sonication Time

The sonication treatment is very common when preparing NFs. For most fluids, the increase of the sonication time contributes to an increase of the thermal conductivity since sedimentation is mitigated and the Brownian motion as well as the particle uniformity improved. Nevertheless, if the sonication time is too long, aggregation decreases and so is the thermal conductivity [5,26]. Hong et al. [65] reported increasing values of thermal conductivity with increasing sonication time until 50 min for ethylene glycol-based iron NFs. Higher sonication values corresponded to a decrease in thermal conductivity. Also, excessive sonication can break NPs with high aspect ratio such as nanotubes [66] and disrupt the effect of the addition of dispersants to the NFs [67].

3.3.6. External Magnetic Field

The NFs can incorporate several magnetically sensitive metal or metal oxide NPs. In such cases, the magnetic particles can have a diversity of configurations depending on the nature of the particles and on the magnetic field magnitude or strength. If the field is strong enough, the small-dimensioned particle will form connected networks or chains that

tend to get oriented toward the magnetic field direction. This alignment effect will move the particles nearby and promotes a larger number of physical contacts and interaction between each other and, thus, resulting in enhanced thermal conductivity and heat transfer capability of the NF. This can be observed in the experimental works performed with Fe_2O_3 or Ni and carbon Nanotubes [68,69]. Also, these studies have demonstrated that as the magnitude of the applied magnet field decreases, the time to reach the maximum peak value of the thermal conductivity will increase.

3.3.7. Aggregation

In recent years, the introduction of carbon nanotubes in NFs has promoted significant research efforts due to their promising enhanced thermal conductivity and, consequently, applications in the cooling and lubricants fields. However, NFs with only a suspension of stand-alone nanotubes do not often exhibit substantially improved thermal conductivity levels. This is likely due to the infrequent physical contacts of the nanotube between each other, as they assume irregular positioning and distribution in the base fluid. To overcome this problem in practice, there are two available ways. One is to increase the volume fraction of the nanotube on the base fluid, which may lead to excessive viscosity of the NF. The other way can be found in the work developed by [70], where the authors proved that the aggregation of oppositely charged NPS (metal oxide and nanotubes) into combined clusters can explain the overall thermal conductivity enhancement. With the proper control of conditions of the suspension itself, it is possible to add fractions of positively charged metal oxide particles on the base fluid that will aggregate on the negatively charged nanotube surface (which is a phenomenon that can be enhanced with the addition of a surfactant) and hence form the aggregation cluster chain along the nanotube by electrostatic attraction.

4. Prediction Models for Thermal Conductivity and Other Properties of the NFs

4.1. Thermal Conductivity Empirical Models

There are a number of prediction models for the conductivity of an NF, based essentially in a weighted average between the properties of the NPs and the base fluid(BF), giving the existing fraction between both [71]. Some of those models were selected to identify the behavior of NFs constituted by spherical particles, with diameters in the order of magnitude that is found in the scope of this work, being the equations presented subsequently. However, many other models can be considered for more specific applications, as it can be found in Lamas [72].

The Maxwell model [73], Equation (1) consists of an empirical model of good approximation and simplicity, for spherical particles in small concentrations. Being one of the first models of this kind, it was widely used as a baseline to other models where additional parameters or corrections were applied.

$$K_{nf\,Maxwell} = K_f \left(\frac{K_{np} + 2K_{bf} + 2\varphi\left(K_{np} - K_{bf}\right)}{K_{np} + 2K_{bf} - 2\varphi\left(K_{np} - K_{bf}\right)} \right) \quad (1)$$

In this equation, as well as in the following ones, K_{nf} corresponds to the NFs thermal conductivity, K_{np} to the NPs thermal conductivity, K_{bf} to the thermal conductivity of the BF,φ to the NP concentration and K_{nf} to the predicted NF thermal conductivity by the used model. Presented by Hamilton and Crosser [72], Equation (2) is based on the same principle, however, it also considers the parameter relative to the shape of the particle. Thus, the shape factor, n, is determined considering the sphericity of the particle, w, as verified in Equation (3) Therefore, the sphericity of the particle varies with the shape, being for instance, for a sphere, $w = 3$, or for a cylinder, $w = 0.5$.

$$K_{nf\,H\&C} = K_{bf} \left(\frac{K_{np} + (n-1)K_{bf} - \varphi(n-1)\left(K_{bf} - K_{np}\right)}{K_{np} + (n-1)K_{bf} + \varphi\left(K_{bf} - K_{np}\right)} \right) \quad (2)$$

$$n = \frac{3}{w} \tag{3}$$

The Wasp prediction model [74], widely used for convection heat transfer problems, is a particular case of the Hamilton and Crosser model, where the particles are perfectly spherical ($w = 1$). Consequently, the Wasp model serves as a good practical approach when there is uncertainty regarding the shape of the particle and can be given by Equation (4):

$$K_{nf\ Wasp} = k_{bf}\left[\frac{k_{np} + 2k_{bf} - 2\varphi\left(k_{bf} - k_{np}\right)}{k_{np} + 2k_{bf} + \varphi\left(k_{bf} - k_{np}\right)}\right] \tag{4}$$

Other model is introduced by Xue [71], that presents a relation between the logarithmic progressions, becoming that way, the most pessimist model for the conductivity gain, as verified in Equation (5):

$$K_{nf\,Xue} = K_{bf}\left(\frac{1 - \varphi + 2\varphi\frac{K_{np}}{K_{np} - K_{bf}} ln\left(\frac{K_{np} + K_{bf}}{2K_f}\right)}{1 - \varphi + 2\varphi\frac{K_f}{K_{np} - K_{bf}} ln\left(\frac{K_{np} + K_{bf}}{2K_{bf}}\right)}\right) \tag{5}$$

The mentioned models are considered static since they ignore the effect of the random movement of the particles in the fluid designated by the Brownian motion. Therefore, to complement the static models, other dynamic models were developed with the purpose of improving the description of mechanisms like the Brownian motion, temperature, size and distribution of the nanoparticles, interfacial layer and cluster formation and morphology that, as we have seen, have crucial effects in thermal conductivity. The dynamic Xuan [75] model uses the Maxwell conductivity model expressed by Equation (1), as a baseline, adding the dynamic effect of the thermal conductivity increase. This model is translated by the Brownian diffusion and clusters formation, translated by Equation (6):

$$K_{nf\,Xuan} = K_{nf\,Maxwell} + \frac{1}{2}\rho_{np} c_{npp} \varphi \sqrt{2D_B} \tag{6}$$

where the Brownian diffusion, D_B, is given by Equation (7), where is possible to verify the effect of temperature, viscosity of the BF and of the clusters, all of them important parameters previously discussed [75]:

$$D_B = \frac{k_B T}{6\pi\mu_{bf} r_c} \tag{7}$$

In this equation, T corresponds to the fluid temperature, r_c corresponds to the average radius of the formed NP clusters, k_B corresponds to the Boltzmann constant and μ_{bf} corresponds to the BF viscosity.

In a similar way, Equation (8) represents the Kleinstreuer model [76], which combines the conductivity according to Maxwell and a term relative to the dynamic conductivity gains.

$$K_{nf\,Kleinstreuer} = K_{nf\,Maxwell} + \frac{5 \times 10^4}{k_{bf}} \beta(\varphi) \rho_{bf} c_{npbf} f(T, \varphi) \sqrt{\frac{k_B T}{\rho_{np} d_{np}}} \tag{8}$$

In this equation it is possible to note a greater diversity of parameters that influence conductivity. Also, the two deducted functions deriving from experimental results reflect the influence of the majority of the aforementioned parameters. The function f, in Equation (9), is designated by factorial function and represents the conductivity effect of the particles, representing parameters like the volume fraction, type of particles, temperature and BF properties. This function was simplified having in consideration only two of the main effects, temperature and volume fraction. The remaining factors are implied in

the result, since the different constants of the equation are obtained by the experimental results analysis.

$$f(T, \varphi) = (-6.04\varphi + 0.4705)T + (1722.3\varphi - 134.63) \quad (9)$$

The function β corresponds to the volume fraction effect, assuming that the remaining parameters dependencies are covered by the function f, being the expression determined having in consideration the large diversity of results with the extra parameters involved, has shown in Figure 4.

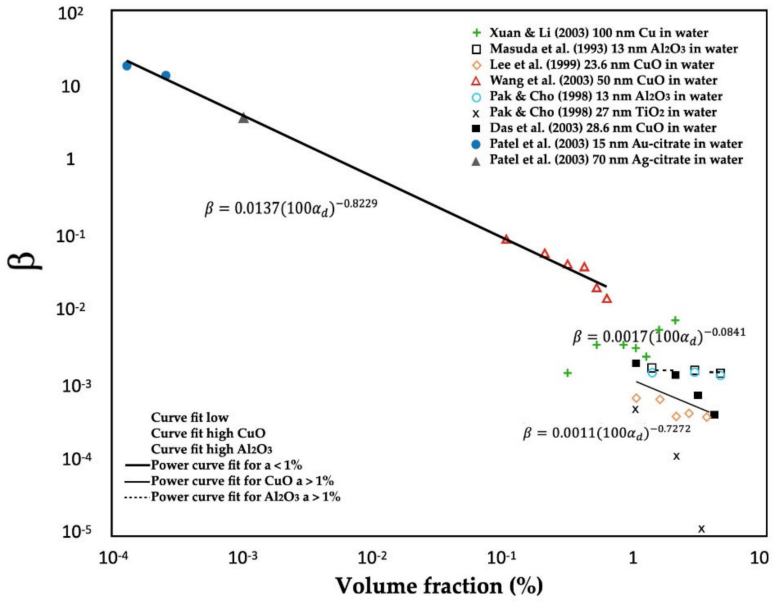

Figure 4. Determination of the function β derived from experimental data, adapted from [76].

Therefore, for the range of volume fractions considered in this scope, the value of β is represented in Equation (10):

$$\beta(\varphi) = 0.0017(100\varphi)^{-0.084} \quad (10)$$

The impact of nanolayer thickness, nanoparticle volume fraction and size and also the thermal conductivity ratio of the nanoparticle to the base fluid were considered in the development of the Xie thermal conductivity prediction model [77], which is given by Equation (11):

$$k_{nf_{Xie}} = 1 + 3\Theta_{\varphi T} + \frac{3\Theta_{\varphi^2 T}^2}{1 - \Theta_{\varphi T}} \quad (11)$$

$$\Theta = \frac{\beta_{lf}\left[(1+\gamma)^3 - \beta_{pl}/\beta_{fl}\right]}{(1+\gamma)^3 + 2\beta_{lf}/\beta_{pl}}, \gamma = \frac{\delta}{r_p} \quad (12)$$

$$\beta_{lf} = \frac{k_l - k_f}{k_l + 2k_f}, \beta_{pl} = \frac{k_p - k_l}{k_p + 2k_l}, \beta_{lf} = \frac{k_f - k_l}{k_f + 2k_l} \quad (13)$$

where δ is the nanolayer thickness and r_p the nanoparticle ratius.

The Table 1 summarizes some of the representative thermal conductivity prediction models and theoretical relations used by the referred researchers.

Table 1. Representative thermal conductivity empirical models (Adapted and abridged from [7,22]).

Researchers	Mathematical Expressions	Included Parameters/Observations
Maxwell [73]	$k_{nf} = K_f\left(\frac{K_{np}+2K_{bf}+2\varphi\left(K_{np}-K_{bf}\right)}{K_{np}+2K_{bf}-2\varphi\left(K_{np}-K_{bf}\right)}\right)$	Includes the thermal conductivities of BF and NPs
Hamilton and Crosser [72]	$k_{nf} = K_{bf}\left(\frac{K_{np}+(n-1)K_{bf}-\varphi(n-1)\left(K_{bf}-K_{np}\right)}{K_{np}+(n-1)K_{bf}+\varphi\left(K_{bf}-K_{np}\right)}\right)$	Includes the particle shape and composition and the thermal conductivities of BF and NPs
Wasp [74]	$k_{nf} = K_{bf}\left(\frac{K_{np}+(n-1)K_{bf}-\varphi(n-1)\left(K_{bf}-K_{np}\right)}{K_{np}+(n-1)K_{bf}+\varphi\left(K_{bf}-K_{np}\right)}\right)$	Includes the thermal conductivities of BF and NPs and the sphericity of the particles assumption
Xue [71]	$k_{nf} = K_{bf}\left(\frac{1-\varphi+2\varphi\frac{K_{np}}{K_{np}-K_{bf}}ln\left(\frac{K_{np}+K_{bf}}{2K_f}\right)}{1-\varphi+2\varphi\frac{K_f}{K_{np}-K_{bf}}ln\left(\frac{K_{np}+K_{bf}}{2K_{bf}}\right)}\right)$	Includes the particle shape and composition and the logarithmic progressions of the thermal conductivities of BF and NPs
Xuan [75]	$k_{nf} = K_{nfMaxwell} + \frac{1}{2}\rho_{np}c_{npp}\varphi\sqrt{2D_B}$	Includes the temperature and viscosity of the BF, the average radius and viscosity of the clusters, and the Brownian motion
Kleinstreuer [76]	$k_{nf} = K_{nfMaxwell} + \frac{5\times10^4}{k_{bf}}\beta(\varphi)\rho_{bf}c_{npbf}f(T,\varphi)\sqrt{\frac{k_BT}{\rho_{np}d_{np}}}$	Includes the temperature and viscosity of the BF, the volume fraction and type of NPs, and the Brownian diffusion
Xie [77]	$k_{nf} = 1 + 3\Theta_{\varphi T} + \frac{3\Theta^2_{\varphi^2 T}}{1-\Theta_{\varphi T}}$	Includes the nanolayer thickness, the NPs volume fraction and radius and the thermal conductivity ratio between the NPs and the BF
Avsec et al. [78]	$k_{nf} = k_{bf}\left[\frac{k_{np}+(n-1)k_{bf}-(n-1)\varphi_{nf}\left(k_{np}-k_{bf}\right)}{k_{np}+(n-1)k_{bf}+\varphi_{nf}\left(k_{np}-k_{bf}\right)}\right]$ $\varphi_{nf} = \varphi\left(1+\frac{h}{r}\right)^3$	Includes the liquid layer thickness, thermal conductivities of BF and NPs, but not the particle size and the interface between the particles
Jang and Choi [32]	$k_{nf} = k_{bf}(1-\varphi) + 0.01k_{nano}\varphi + 18\times10^6\frac{d_{bf}}{d_{np}}\cdot k_{bf}Re_d^2Pr_{bf}\varphi$	Includes the thermal condutivity and the diameter of the molecules of the BF, the particle fraction and diameter, the thermal conductivity of the NPs involving the Kapitza resistance (surface resistance),and the numbers of Reynolds and Prandtl
Pak and Cho [79]	$k_{nf} = 1 + 7.47\varphi$	Includes the geometry, diameter, and the surface resistance of the NPs
Timofeeva et al. [33]	$k_{nf} = k_f(1+3\varphi)$	Includes the geometry, agglomeration state, and the surface resistance of the NPs
Yu and Choi et al. [80]	$k_{nf} = k_{bf}\left[\frac{k_{pe}+2k_{bf}+2\left(k_{pe}-k_{bf}\right)(1+\beta)^3\varphi}{k_{pe}+2k_{bf}-\left(k_{pe}-k_{bf}\right)(1+\beta)^3\varphi}\right]$ $k_{pe} = k_{np}\left[\frac{[2(1-\gamma)+(1+\beta)^3(1+2\gamma)]\gamma}{-(1-\gamma)+(1+\beta)^3(1+2\gamma)}\right]$	Modified Maxwell model.Includes the nanolayer thickness
Wang et al. [81]	$k_{nf} = k_{bf}\left[1+\frac{\frac{3f_q(p)}{p_0}}{1-\frac{f_q(p)}{p_0}}\right]$	Includes nanolayer thickness, particle size, temperature, volume fraction, and interaction between adjacent particles
Chandrasekar et al. [82]	$MODEL\ I: k_{nf} = k_{bf}\left[\left(\frac{c_{np,\,nf}}{c_p}\right)\left(\frac{\rho_{nf}}{\rho}\right)^{1.33}\left(\frac{M}{M_{nf}}\right)^{0.33}\right] MODEL\ II: k_{nf}$ $= k_{bf}\left[\frac{k_{np}+(n-1)k_{bf}+(n-1)\left(k_{np}-k_{bf}\right)(1+\beta)^3\varphi}{k_{np}+(n-1)k_{bf}-\left(k_{np}-k_{bf}\right)(1+\beta)^3\varphi}\right]$	Model I is applicable over a wide range of particlenature, fraction and size, and different base fluids. Model II help to determine the contribution layer thickness, particle shape, and Brownian motion
Corcione [83]	$k_{nf} = 1 + 4.4Re^{0.4}Pr^{0.66}\left(\frac{T}{T_{fre}}\right)^{10}\cdot\left(\frac{k_{np}}{k_{bf}}\right)^{0.03}\cdot\varphi^{0.66}$	Applicable for the temperature range of 294–324 K, nanoparticle diameter of 10–150 nm and volume fraction of 0.002–0.9

In general terms, the behavior of some of the different models for conductivity prediction are represented in the Figure 5, having in consideration some calculation simplifications, like the type of particles, temperature, presence of clusters, and their dimension. As it can be noted, the behavior of the models is in line with what is expected, that is, the dynamic models are the ones that present a greater thermal conductivity, since they have the Brownian motion in consideration, being the increment linear in all of the models, excepting the Kleinstreuer model, where the influence of the volume fraction is more relevant.

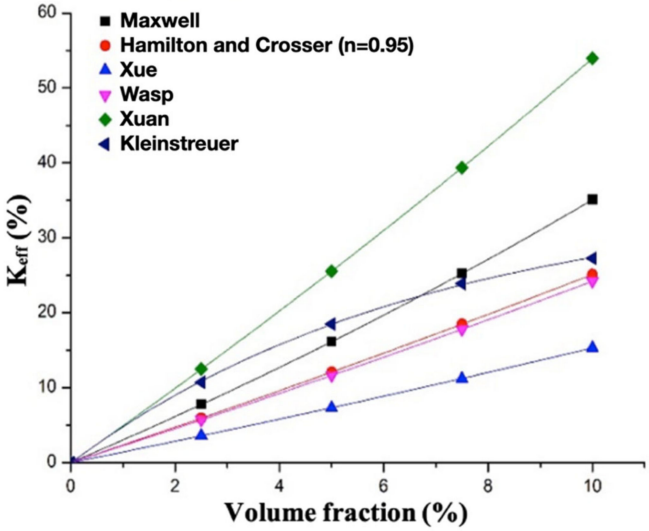

Figure 5. Behavior of the different models for thermal conductivity prediction of an NF in function of the nanoparticle(NP) fraction [84].

4.2. Thermal Conductivity Machine Learning-Based Models

In recent years, many machine learning and statistical models has been developed to predict the thermal conductivity and other thermal properties of materials and nanofluids with high accuracy and robustness. In fact, properties such as thermal conductivity [85], density [86], and viscosity [87,88] of nanofluids, glass transition temperature of polymers [89,90] and also the decomposition onset temperature of lubricant additives [91] have been estimated precisely with machine learning-based models. Those models are fast, stable, and low-cost tools to predict the thermal properties on a wide range of industrial applications, particularly in electronic devices, heat sinks, heat exchangers, renewable energy [92], and automotive industries. Accordingly, there are also many research works whose predictions were based in machine learning algorithms, as can be seen in Table 2, which summarizes representative papers using machine learning prediction models published in recent years.

The most common machine learning data-driven modeling can be provided by one of these four fundamental models: ANN (Artificial Neural Network), CART (Category and Regression Tree), RF (Random Forest), and SVM (Support Vector Machine). The chart presented in Figure 6 shows these fundamental methods and their possible combinations like, for instance, GA (Genetic Algorithm) and PSO (Particle Sworn Optimization). Figure 7 illustrates the structure of an ANN estimation model, which is the most commonly used model in the research field.

4.3. Density

The determination of the density of the NFs can be made through the use of a simple weighted average of the isolated properties of the NPs and the BF, having in consideration the volume fraction, as demonstrated in Equation (14) [3]:

$$\rho_{nf} = \rho_p \varphi + \rho_{bf}(1 - \varphi) \quad (14)$$

φ corresponds to NP concentration, ρ_p to NP density, ρ_{nf} to NF density and ρ_{bf} to BF density.

Table 2. Representative review papers on nanofluid heat transfer research using machine learning prediction models.

Reference	Work Focus	Machine Learning Involvement
Zhao et al., 2016 [93]	Prediction of thermal conductivity and viscosity based on ANN and applications in automotive radiators	ANN data-driven modeling
Ramezanizadeh et al., 2019 [94]	Characteristics of different machine learning methods including MLP-ANN, GMDH, ANFIS, RBF, and LS-SVM combined with GA, PSO, and ICA. Applications of machine learning methods to dynamic viscosity modeling of nanofluids	Machine learning for viscosity prediction
Bahiraei et al., 2019 [95]	AI algorithms inluding ANNs, fuzzy logic optimization methods and hybrid AI algorithms used for prediction and optimization of thermal properties of nanofluids	Machine learning algorithms for prediction and optimization
Guo 2020 [96]	Overview on measured thermal properties, enhancement mechanisms, models for properties and heat transfer characteristics and applications of nanofluids to cooling, renewable energy, and energy and building technologies	ANN model for thermal conductivity prediction
Sahaluddin et al., 2020 [86]	Development of a machine learning model for density prediction of nitrides in ethylene glycol. The developed is much more accurate than the Pak and Cho empirical model	SVM model for density prediction
Zhang and Xu 2020 [89]	Machine learning glass transition temperature of polymers prediction using a GPR (*Gauss Process Regression*) data-driven model	GPR model for glass transition temperature prediction
Zhang and Xu 2020 [91]	Machine learning decomposition onset temperature of lubricant additives prediction using a GPR data-driven model	GPR model for temperature prediction
Shateri et al., 2020 [88]	CMIS (*Comittee Machine Intelligent System*) machine learning model for nanofluid viscosity estimation	CMIS model for viscosity prediction
Alade et al., 2020 [87]	BSVR (*Bayesian Support Vector Regression*) and ANN machine learning models for nanofluid viscosity prediction	BSVR and ANN models for viscosity prediction
Ma et al., 2021 [92]	Nanofluid heat transfer machine learning research applied to renewable energy	Machine learning description and applications

4.4. Specific Heat Capacity

In a similar way to what was previously presented for the density, the specific heat capacity can also be determined in the same way, using Equation (15). The values obtained through this method are very similar to the BF. However, further experimental tests are required to improve the theoretical approaches [3]:

$$C_{pnf} = \frac{\varphi \rho_p C_{pnp} + (1 - \varphi)\rho_{bf} C_{pbf}}{\rho_{nf}} \quad (15)$$

Here C_{pbf} corresponds to BF specific heat capacity, C_{pnp} to NP specific heat capacity and C_{pnf} to NF specific heat capacity.

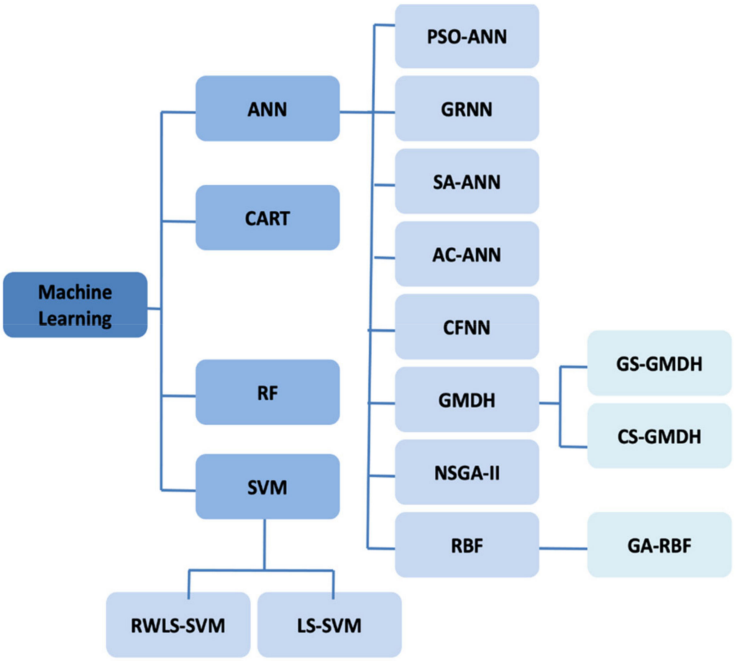

Figure 6. Categories of prediction and regression machine learning algorithms (Adapted and abridged from [92].

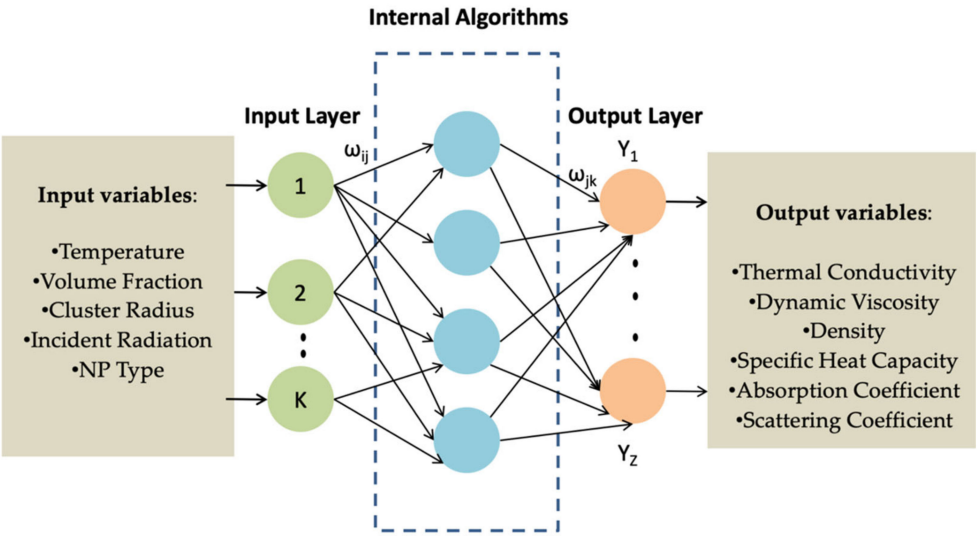

Figure 7. Schematic structure of the Artificial Neural Network (ANN) machine learning model topology (Adapted and abridged from [92]).

4.5. Viscosity

The treatment of the viscosity variation in an NF can be considered similar to the effect in the viscosity of a solvent by adding particles of a solute. As in the conductivity study, there is a predominant model for the viscosity that was undergone to corrections over time. This model is designated by Einstein model, which in 1906, precisely studied the phenomenon of particle diffusion in a solute of a diluted solution. For that purpose, based in the Navier-Stokes equation for an incompressible flow, we can have Equation (16):

$$\mu_{nf} = (1 + \varepsilon\varphi)\mu_{bf} \tag{16}$$

In this equation, φ corresponds to the used NP concentration and μ_{fb} and μ_{nf} to the NF viscosities and BF, respectively. We can observe the existence of the factor ε that

will be representative of the type of particles in the solute. Considering them as rigid spheres, disregarding the interactions between them and with much bigger dimensions than the solvent particles, the factor will be 2.5, making Equation (17) valid for a certain concentration range:

$$\mu_{nf} = (1 + 2.5\varphi)\mu_{bf} \quad , \ 0 < \varphi < 10\% \tag{17}$$

As it has been discussed throughout this section, the interaction between the particles is a fundamental mechanism of the behavior of the NFs. In the latter, Pavlik [97] has proposed a new equation that introduces a quadratic dependence with the volume fraction that allows a better representation of the particle interaction, as shown by Equation (18) and valid for the same interval:

$$\mu_{nf} = \left(1 + 2.5\varphi + 6.2\varphi^2\right)\mu_{bf} \quad , \ 0 < \varphi < 10\% \tag{18}$$

Other models present alternative calculation methods to the Einstein deduction, as the case of Brinkman [98], Brandy, or Krieger-Dougherty in [97]. This model was presented by Mooney [99] and presents an exponential progression to explain the observed rise in viscosity, as it is reported in Equation (19):

$$\mu_{nf} = \mu_{bf} e^{\frac{2.5\varphi}{1-k\varphi}} \tag{19}$$

This factor k here introduced is designated by self-crowding effect, that better represents the interaction between particles, especially in greater concentrations, being the particle movement hampered by the existence of a greater number of neighbor particles, approximating their behavior to a solid. This factor k increases withparticle concentration, having the author estimated that the factor would belong in the range $1.35 < k < 1.91$.

5. Controversies in Thermal Conductivity Measurements

A large variety of techniques and devices to measure the thermal conductivity of NFs can be commonly found in the literature. Although some of the devices may be more sophisticated than others, they all converge on a common problem: they are very sensitive and dependent on the initial conditions of the samples. Even for minimal variations, the results can promote a strong impact on the final conclusions. Most of the techniques presented in this work have been adapted over the years to be able to safely measure the thermal conductivity of NFs. This task has not been easy due to the difficulty of maintaining the stability of the samples. The dispersion techniques proposed by recent research studies [100] can achieve months of stability, but the recurring necessity of continuous maintenance and the gradual sedimentation of the nanoparticles throughout the system can help us understand the reason for so many controversial results.

Another reported difficulty is associated with the concentration of the NPs in the BF. Even though the results have not yet reached a general consensus, the simplest solution found by the majority of the researchers to increase the gains in thermal conductivity of colloidal mixtures is to increase the concentration of NPs in the BF. However, as the concentration of the NPs increases, NF viscosity also increases, leading to flow resistance. The greater viscosity of those fluids increases power requirements of the pumping system and pressure losses in the case of heat sinks, when compared to the respective base fluids.

Another property that can affect the measurement of the thermal conductivity of NFs is the specific heat of all their components, that is, the BFs, NPs and dispersants used. This property relevance and its effects are also not unanimous among the scientific community and are not yet fully understood. The high specific heat of water is the main reason why it is used as cooling fluid in a large variety of applications, even when compared to other fluids. In this way, it is possible to provide a high amount of energy, without promoting a high increase of temperature at the systems. On the other hand, the NPs used to form the colloidal mixtures have a lower specific heat, and this lower contribution of the NPs to the NF heat capacity needs to be compensated. For example, Nieh et al. [101], using

an NF formed by NPs ofAl_2O_3 or TiO_2 prepared with ethylene glycol/water, studied the effect of adding a dispersant to evaluate the influence in the specific heat. They observed an increase of the specific heat but, it was gradually decreased with the increase of wt% of Al_2O_3 and TiO_2. Without addition of the dispersants, some researchers have shown that the specific heat of NFs decreases with the increase of volume fraction [101–103].

The potential of NFs to increase the heat transfer capacity of thermal systems is accepted by a large part of the scientific community. However, the lack of consistent results obtained by different researchers has hampered the development of this field and the use of NFs in large scale industrial applications. The poor characterization of the suspensions of NPs and the lack of theoretical understanding of the mechanisms responsible for thermal properties changes need further understanding. Many issues besides the thermal conductivity, such as the Brownian motion and sedimentation of NPs, particle migration, and temperature-dependent properties, must be carefully considered, especially when the thermal analysis involve not only natural but also convective heat transfer phenomena within the nanofluid. The Table 3 shows the measurements of thermal conductivity for a series of NFs using different techniques addressed in this study.

Table 3. Thermal conductivity enhancement measurements for different nanofluids (NFs).

NPs	BF	Size [nm]	Concentration	K_{eff} Increase [%]	Method	Ref.
Al_2O_3	Water	33	1 and 2 vol.%	5.4	Theory	[104]
		30–60	0.5, 1.0, 2, 3 and 4 vol.%	1.96	THW	[105]
		10, 20–30 and 150	Up to 1.5 vol.%	23	Theory	[106]
		13	0.1, 0.15, 0.20 and 0.25 vol.%	6.40 for 0.25 vol.% NF	THW	[107]
		41	18 vol.%	31	THW	[54]
		36	10 vol.%	30	SSCB	[108]
		36	6 vol.%	28	SSCB	[109]
		20	14.6 vol.%	22	TSHW	[110]
		282	4 vol.%	17.7	THW	[111]
		40	4 vol.%	14.4	Flash	[112]
		15–50	4 vol.%	10.1	TPS	[61]
		43	3 vol.%	9.7	THW	[113]
		11	1 vol.%	9	THW	[53]
		38	3 vol.%	8	THW	[114]
		43	2 vol.%	7.52	THW	[113]
		10	0.08 vol.%	7.1	THW	[115]
		12	4 vol.%	5.4	THW	[116]
		10	0.05 vol.%	4.7	THW	[115]
		43	0.75 vol.%	3.28	THW	[113]
		10	0.04 vol.%	3.1	THW	[115]
		43	0.33 vol.%	1.64	THW	[113]
	EG	10	0.08 vol.%	22	THW	[115]
		10	0.06 vol.%	17.3	THW	[115]
		282	3 vol.%	16.3	THW	[111]
		12	4 vol.%	14.3	THW	[116]
		38	3 vol.%	10.6	THW	[114]
		45	4 vol.%	9.7	3ω	[117]
		13	2 vol.%	12.6	THW	[118]
	EG/Water	10	3 vol.%	11.3	THW	[116]
		50	3 vol.%	10.4	THW	[116]
		13	2 vol.%	8.4	THW	[118]
		13	2 vol.%	16.2	THW	[118]
	DI	45	4 vol.%	13.3	3ω	[117]
		48	1 vol.%	4	THW	[28]

Table 3. *Cont.*

NPs	BF	Size [nm]	Concentration	K_{eff} Increase [%]	Method	Ref.
TiO_2	Water	21	0.1 vol%	About 11.1	THW	[119]
		100	0.10, 0.15, 0.21 and 0.25 vol.%	16.7 for TiO_2-0.25%	THW	[120]
		10, 30, and 50	0.005, 0.01, 0.1, 0.5, and 1 vol.%	0.4	Theory	[121]
		5	0, 0.1, 0.5 and 1.0 vol.%	6.55	TPS	[122]
		21	0.1–0.5 vol.%	7.28		[123]
		10	3 vol.%	11.4	THW	[114]
		34	3 vol.%	8.7	THW	[114]
		21	2 vol.%	7	THW	[56]
		40	2.6 vol.%	6.5	THW	[110]
		70	3 vol.%	6.4	THW	[114]
		20	2 vol.%	4.2	THW	[124]
	Water:EG	40	0.2 to 0.8 vol.%	24 at VF 0.8% and temperature 50 °C	THW	[125]
	EG	5	7 vol.%	19.52	THW	[126]
		15	5 vol.%	18	THW	[127]
		10	3 vol.%	14.4	THW	[114]
		34	3 vol.%	12.3	THW	[114]
		70	3 vol.%	7.5	THW	[114]
	DI	Ø10×40	5 vol.%	33	THW	[34]
		15	5 vol.%	30	THW	[34]
		20.5	1 vol.%	14.4	THW	[28]
SiC	Water	21	3 vol.%	7.2	3ω	[128]
		45–65	1, 1.5, 2, 3, and 4 wt%	8.2	THW	[129]
		45–65	0.5, 1.0, 2, 3 and 4 vol.%	4.8	THW	[105]
		35–45	0.5, 1.0, 2, 3 and 4 vol.%	3.42	THW	[105]
CuO	Water	29	6 vol.%	52	SSCB	[108]
		25	7.5 vol.%	32.3	THW	[130]
		55–66	2 vol.%	24	THW	[129]
		33	4.68 vol.%	16.5	TSHW	[131]
		33	1 vol.%	5	THW	[131]
	Water + 0.5 wt% CMC	40	0.2–1.0 wt%	29%	THW	[132]
	EG	55–66	2 vol.%	21	THW	[130]
		33	1 vol.%	9	THW	[40]
	MEG	25	7.5 vol.%	21.3	THW	[129]
	EO	55–66	2 vol.%	14	THW	[130]
CeO_2	EG	10–30	2.5 vol.%	22	THW	[132]
ZnO	Water	10	3 vol.%	14.2	THW	[133]
		60	3 vol.%	7.3	THW	[134]
	EG	30	3 vol.%	21	THW	[113]
		50	2.4 vol.%	13	THW	[135]
WO_3	EG	38	0.3 vol.%	13.8	THW	[28]
Fe_3O_4	Kerosene	15	1 vol.%	34.6	THW	[136]
	Water	15–23	3 vol.%	11.5	THW	[137]
		15–20	4.8 vol.%	2.9	3ω	[138]
		15–20	1 vol.%	1.1	3ω	[138]
$NiFe_2O_4$	DI	8	2 vol.%	17.2	THW	[139]
MgO	EG/Water	40	3 vol.%	34.43	THW	[140]
Cu	Water	75–100	0.1 vol.%	23.8	THW	[141]

Table 3. *Cont.*

NPs	BF	Size [nm]	Concentration	K_{eff} Increase [%]	Method	Ref.
Au	Toluene	1.65	0.003 vol.%	8	TSHW	[110]
		2	0.024 vol.%	1.4	MSBD	[142]
	Ethanol	4	0.018 vol.%	1.3	MSBD	[142]
Ag	Water	96	1.7×10−5 vol.%	20.8	TWRC	[143]
		96	3.5×10−6 vol.%	4	TWRC	[143]
Fe	DI	5–25	0.5 vol.%	16	THW	[144]
	EG	20	4 vol.%	38.8	Theory	[145]
		10	0.55 vol.%	18	THW	[64]
		10	0.3 vol.%	16.5	THW	[28]
		50	2 vol.%	15.5	Theory	[145]
Al	EG	80	5 vol.%	45	THW	[127]
SiC (sphere)	DI	100	3 vol.%	7.2	THW	[146]
	DO	30	0.8 vol.%	7.36	THW	[147]
SiO_2	Water	40–50	3 vol.%	38.2	THW	[148]
		12	1 vol.%	3.2	THW	[132]
		12	1 vol.%	3	THW	[40]
MgO/TiO_2	Water	10–45	50:50, 80:20, 20:80, 60:40 and 40:60 wt%	21.8 at 50 °C	THW	[149]
Graphene nanoplatelet (GFnanopl)	Water		0.025 to 0.1 wt%	27	THW	[150]
	EG	0.7–1.3	0.05vol.%	86	TSHW	[151]
Graphene Oxide	EG	0.7–1.4	0.05vol.%	61	TSHW	[151]
GFnanopl – SDBS	Water		0.025, 0.05 and 0.1 wt.%	About 11.56	Theory	[152]
GFnanopl – COOH	Water		0.025, 0.05 and 0.1 wt.%	About 21.03	Theory	[152]
Al_2O_3 — MWCNT	Water	10–100 (Al_2O_3)	0.01 vol.%	10.85 for MWCNT (0:5) NFs	THW	[153]
MWCNT	Solar glycol	20–30	0.2, 0.4, and0.6 vol.%	30.59 with MWCNT volume of 0.6%	THW	[154]
	Jatropha seed oil	Length × OD = 2.5–20 µm × 6–13nm	0.2–0.8 wt.%	6.76	THW	[155]
	Water	Ø40	0.49 vol.%	80	THW	[156]
		Ø130	0.6 vol.%	34	THW	[157]
		Ø10–30	1 vol.%	7	THW	[132]
		Ø10–30	0.48 vol.%	5	THW	[158]
	HTO	Ø5–20	2 vol.%	15	THW	[159]
	EG	Ø20–50	1 vol.%	12.4	THW	[160]
	EO	Ø20–50	1 vol.%	8.5	THW	[160]
DWCNT	Water	Ø5	1 vol.%	8	THW	[157]
SWCNT	Water	Ø1-2×5000-30,000	0.48 vol.%	16.2	THW	[157]
		Ø1-2×1000–3000	0.48 vol.%	8.1	THW	[158]
	EG	100–600	0.21 vol.%	15.5	THW	[161]
C60-C70 fullerenes	Toluene	–	0.378 vol.%	0.816	MSBD	[143]
	MO	10	5 vol.%	6	THW	[132]

Legend: BF = Base Fluid; K_{eff} = Effective thermal conductivity; THW = Transient Hot-Wire; SSCB = Steady state "cut bar"; TSHW = Transient Short Hot-Wire; TPS = Transient Plane-Source; MSBD = Micronscale Beam Deflection Technique; TWRC = thermal-wave resonator cavity.

6. Backdraws and Future

The backdraws, difficulties and general limitations of the NFs can be summarized in the following points:

- Complexity and high cost of NFs preparation;
- Long-term stable NFs are difficult to produce. The influence of the production should be further studied, namely the sonication time, volume fraction, and type of the NFS in order to avoid the sedimentation and agglomeration of the NPs in the BF and to achieve optimal performance;
- Lack of a common protocol for the manufacture and analysis of the thermal transport mechanisms in this type of fluids;
- Methods to scale-up production for commercialization are still in development;
- Some of the classical experimental fitting prediction models for thermal properties are not the most suitable for the estimation of the thermal conductivity, dynamic viscosity and density of the NFs;
- The classical modeling does not provide a fast prediction of the thermal properties, which may slow down the study and overall applicability of the NFs;
- Nowadays, it is clear the need to use the recent statistical data-driven machine learning models to obtain faster predictions of the thermal properties of the NFs. Those models are also more stable and sensitive than the empirical ones. However, for a in-depth knowledge on how the recent models work, the researchers must get proficient skills in machine learning methodology and in the most common data-driven models and algorithms;
- The proper machine learning model and algorithms should be chosen according to the dimension of the sample, the available computing resources, and the required prediction performance (modeling stability and sensibility).

By way of guidelines that might be the path for future challenges and further studies and developments, the authors of the current work wish to emphasize the following:

- The stability and durability of the nanofluids should be improved by optimizing the concentration of NPs and base fluid characteristics (e.g., chemical, viscosity). The stability of nanofluids should also be predicted by further analysis of the surface tension of the nanofluid vs. time;
- The general properties of the NFs should be improved by optimizing the preparation procedures (e.g., sonication time);
- The influence of the solvents should be further studied: the use of high polar solvents like the DMF (Dimethylformamide) and THF (Tetrahydrofuran) and non-polar solvents as hexane and heptane could be the right way to fully understand how polarity influences the alignment and thermal conductivity of the NFs;
- The influence of the polarity in the alignment of the NPS on the base fluid can also be assessed by the use of different surfactants with negative charge, such as for instance CATB (Cetyltrimethylamonium bromide);
- The impact of an applied magnetic field should be further studied, namely the value or range of values that make possible to reach the thermal conductivity maximum peak in less time;
- Additives for decreasing the NFs viscosity while maintaining the same level of thermal conductivity are of paramount importance to achieve the best performance of the NFs;
- The systems using nanofluids as working fluid should become more cost-effective, without the need of extra pumping power and expensive maintenance. This should be accomplished with the optimization of the microchannels configuration (e.g. number of channels, inlet/outlet positioning);
- Machine learning prediction models should be increasingly used in the future, since they provide faster and less expensive modeling of thermal properties of the NFs. Those data-driven models achieve more accurate and stable estimations than the classical ones. The path created by machine learning is beginning to clear up several doubts and backdraws, and it is a secure one for future studies and developments on the nanomaterials field of research.

7. Conclusions

From all the results and discussions shown in this literature review, it is clear that the benefits of nanofluids are vast, since they can be used in a wide variety of applications from nanomedicine to renewable energies. Due to their superior thermal properties, nanofluids have become protagonists in increasing the heat transfer from the thermal systems as their use very suitable to miniaturize fluidic systems. Although the series of studies presented by the scientific community are not always consistent, several results generally converge on the same conclusions, as follows:

- the thermal conductivity of an NF is greater than the one of the respective base fluids;
- the methods used to measure the thermal properties of NFs are still in an embryonic stage of development;
- the heat transfer coefficient of an NF is higher than the one of the respective base fluid;
- viscosity of NFs increases with the concentration of the NPs leading to higher pumping power requirements;
- NF long-term stability is mandatory for miniaturized fluidic systems, mainly mini or microchannels devices;
- the production costs for systems using nanofluids as working fluid are still high.

Author Contributions: Conceptualization, A.M.(Ana Moita), J.M., J.E.P., G.C. and R.S.; methodology, A.M.(Ana Moita), J.M., J.E.P., G.C. and R.S; formal analysis, A.M.(Ana Moita), J.M., J.E.P., G.C., R.S and I.G.; investigation, A.M.(Ana Moita), J.M., R.S, I.G., J.E.P. and G.C., resources, A.M.(Ana Moita), J.M., R.S and A.M.(António Moreira), data curation, R.S. and I.G., writing-original drafting preparation, A.M.(Ana Moita), J.E.P., G.C., R.S and I.G., writing-review and editing, A.M.(Ana Moita), J.M.,R.L., R.S., J.E.P., A.M.(António Moreira) and G.C.; visualization, A.M.(Ana Moita), J.M., J.E.P., G.C., R.S., supervision, R.L., A.M.(Ana Moita) and J.M.; project administration, A.M.(Ana Moita), J.M. and A.M.(António Moreira), funding acquisition, R.L., A.M.(Ana Moita), J.M. and A.M.(António Moreira). All authors have read and agreed to the published version of the manuscript.

Funding: This research received no external funding.

Data Availability Statement: The data supporting reported results presented in Figure 1 is available online at: https://www.sciencedirect.com/search?qs=nanofluids. (Accessed on 12 January 2021).

Acknowledgments: This work has been funded by Portuguese national funds of FCT/MCTES (PIDDAC) through the base funding from the following research units: UIDB/00532/2020 (Transport Phenomena Research Center–CEFT), UIDB/04077/2020 (MEtRICs) and UIDP/04436/2020.The authors are also grateful for the funding of FCT through the projects POCI-01-0145-FEDER-016861, POCI-01-0145-FEDER-028159, NORTE-01-0145-FEDER-029394, NORTE-01-0145-FEDER-030171, funded by COMPETE2020, NORTE2020, PORTUGAL2020, and FEDER.

Conflicts of Interest: The authors declare no conflict of interest.

Abbreviations

AC-ANN	Ant Colony Artificial Neural Network
ANN	Artificial Neural Network
CART	Category and Regression Tree
CS-GMDH	Group Method of Data Handling
CFNN	Correlation Filter Neural Network
GA-RBF	Genetic Algorithm Radial Basis Function
GMDH	Group Method of Data Handling
GRNN	General Regression Neural Network
GS-GMDH	Generalized Structure Group Method of Data Handling
LS-SVM	Least Square Support Vector Machine
NSGA II	Non-dominated Sorting Genetic Algorithm
PSO-ANN	Particle Sworn Optimization Artificial Neural Network

RBF	Radial Basis Function
RF	Random Forest
RWLS-SVM	Recursive Weighted Least Squares Support Vector Machine
SA-ANN	Simulate Anneal Artificial Neural Network
SVM	Support Vector Machine

References

1. Garimella, S.V.; Persoons, T.; Weibel, J.A.; Gektin, V. Electronics Thermal Management in Information and Communications Technologies: Challenges and Future Directions. *IEEE Trans. Compon. Packag. Manuf. Technol.* **2016**, *7*, 1191–1205. [CrossRef]
2. Ghadimi, A.; Saidur, R.; Metselaar, H.S.C. A review of nanofluid stability properties and characterization in stationary conditions. *Int. J. Heat Mass Transf.* **2011**, *54*, 4051–4068. [CrossRef]
3. Pang, C.; Lee, J.W.; Kang, Y.T. Review on combined heat and mass transfer characteristics in nanofluids. *Int. J. Therm. Sci.* **2015**, *87*, 49–67. [CrossRef]
4. Younes, H.; Christensen, G.; Li, D.; Hong, H.; Ghaferi, A.A. Thermal Conductivity of Nanofluids: Review. *J. Nanofluids* **2015**, *4*, 107–132. [CrossRef]
5. Qiu, L.; Zhu, N.; Feng, Y.; Michaelides, E.E.; Żyła, G.; Jing, D.; Zhang, X.; Norris, P.M.; Markides, C.N.; Mahian, O. A review of recent advances in thermophysical properties at the nanoscale: From solid state to colloids. *Phys. Rep.* **2020**, *843*, 1–81. [CrossRef]
6. Elcock, D. *Potential Impacts of Nanotechnology on Energy Transmission Applications and Needs*; Environmental Science Division; Argonne National Laboratory: Argonne, Il, USA, 2007.
7. Ali, H.M.; Babar, H.; Shah, T.R.; Sajid, M.U.; Qasim, M.A.; Javed, S. Prepartion Techniques of TiO2 Nanofluids and Challenges: A Review. *Appl. Sci.* **2018**, *8*, 587.
8. Maia, I.; Rocha, C.; Pontes, P.; Cardoso, V.M.; Miranda, J.S.; Moita, A.; Minas, G.L.N.; Moreira, A.; Lima, R. Heat Transfer and Fluid Flow Investigations in PDMS Microchannel Heat Sinks Fabricated by Means of a Low-Cost 3D Printer. In *Advances in Microfluidic Technologies for Energy and Environmental Applications*; IntechOpen: London, UK, 2020.
9. Freitas, E.; Pontes, P.; Cautela, R.; Bahadur, V.; Miranda, J.; Ribeiro, A.P.C.; Souza, R.R.; Oliveira, J.D.; Copetti, J.B.; Lima, R.; et al. Pool Boiling of Nanofluids on Biphilic Surfaces: An Experimental and Numerical Study. *Nanomaterials* **2021**, *11*, 125. [CrossRef] [PubMed]
10. Nagpal, S. Nanofluids to be used to make new types of cameras, microdevices, and displays. Available online: https://topnews.in/nanofluids-be-used-make-new-types-cameras-microdevices-and-displays-221378 (accessed on 12 January 2021).
11. Serrano, E.; Rus, G.; García-Martínez, J. Nanotechnology for sustainable energy. *Renew. Sustain. Energy Rev.* **2009**, *13*, 2373–2384. [CrossRef]
12. Saidur, R.; Leong, K.Y.Y.; Mohammed, H.A.A. A review on applications and challenges of nanofluids. *Renew. Sustain. Energy Rev.* **2011**, *15*, 1646–1668. [CrossRef]
13. Buongiorno, J.; Hu, L.-W. *8. Innovative Technologies: Two-Phase Heat Transfer in Water-Based Nanofluids for Nuclear Applications Final Report*; Massachusetts Institute of Technology: Cambridge, MA, USA, 2009.
14. Kuo, K.K.; Risha, G.A.; Evans, B.J.; Boyer, E. Potential Usage of Energetic Nano-sized Powders for Combustion and Rocket Propulsion. *MRS Proc.* **2003**, *800*, AA1.1. [CrossRef]
15. Srikant, R.R.; Rao, D.N.; Subrahmanyam, M.S.; Krishna, P.V. Applicability of cutting fluids with nanoparticle inclusion as coolants in machining. *Proc. Inst. Mech. Eng. Part J. J. Eng. Tribol.* **2009**, *223*, 221–225. [CrossRef]
16. Wilson, C.A. Experimental Investigation of Nanofluid Oscillating Heat Pipes. Ph.D. Dissertation, University of Missouri, Columbia, MO, USA, 2006.
17. Grab, T.; Gross, U.; Franzke, U.; Buschmann, M.H. Operation performance of thermosyphons employing titania and gold nanofluids. *Int. J. Therm. Sci.* **2014**, *86*, 352–364. [CrossRef]
18. Tyagi, H.; Phelan, P.; Prasher, R. Predicted efficiency of a Low-temperature Nanofluid-based direct absorption solar collector. *J. Sol. Energy Eng. Trans. ASME* **2009**, *131*, 0410041–0410047. [CrossRef]
19. Demetzos, C. Application of Nanotechnology in Imaging and Diagnostics. In *Pharmaceutical Nanotechnology: Fundamentals and Practical Applications*; Springer: Singapore, 2016; pp. 65–75, ISBN 978-981-10-0791-0.
20. Rodrigues, R.O.; Sousa, P.; Gaspar, J.; Bañobre-López, M.; Lima, R.; Minas, G. Organ-on-a-chip: A Preclinical Microfluidic Platform for the Progress of Nanomedicine. *Small* **2020**, 2003517. [CrossRef] [PubMed]
21. Kung, C.T.; Gao, H.; Lee, C.Y.; Wang, Y.N.; Dong, W.; Ko, C.H.; Wang, G.; Fu, L.M. Microfluidic synthesis control technology and its application in drug delivery, bioimaging, biosensing, environmental analysis and cell analysis. *Chem. Eng. J.* **2020**, *399*, 125748. [CrossRef]
22. Rostami, S.; Aghakhani, S.; Pordanjani, A.H.; Afrand, M.; Cheraghian, G.; Oztop, H.F.; Shadloo, M.S. A review on the Control Parameters of Natural Convection in Different Shaped Cavities with and without nanofluids. *Processes* **2020**, *8*, 1011. [CrossRef]
23. Gupta, M.; Singh, V.; Kumar, R.; Said, Z. A review on thermophysical properties of nanofluids and heat transfer applications. *Renew. Sustain. Energy Rev.* **2017**, *74*, 638–670. [CrossRef]
24. Xu, G.; Fu, J.; Dong, B.; Quan, Y.; Song, G. A novel method to measure thermal conductivity of nanofluids. *Int. J. Heat Mass Transf.* **2019**, *130*, 978–988. [CrossRef]

25. Bhattacharya, P.; Nara, S.; Vijayan, P.; Tang, T.; Lai, W.; Phelan, P.E.E.; Prasher, R.S.S.; Song, D.W.W.; Wang, J. Characterization of the temperature oscillation technique to measure the thermal conductivity of fluids. *Int. J. Heat Mass Transf.* **2006**, *49*, 2950–2956. [CrossRef]
26. Philip, J.; Shima, P.D. Thermal properties of nanofluids. *Adv. Colloid Interface Sci.* **2012**, *183–184*, 30–45. [CrossRef]
27. Wang, X.; Zhu, D.; Yang, S. Investigation of pH and SDBS on enhancement of thermal conductivity in nanofluids. *Chem. Phys. Lett.* **2009**, *470*, 107–111. [CrossRef]
28. Yoo, D.-H.; Hong, K.S.; Yang, H.-S. Study of thermal conductivity of nanofluids for the application of heat transfer fluids. *Thermochim. Acta* **2007**, *455*, 66–69. [CrossRef]
29. Ambreen, T.; Kim, M.H. Influence of particle size on the effective thermal conductivity of nanofluids: A critical review. *Appl. Energy* **2020**, *264*. [CrossRef]
30. Xu, J.; Yu, B. A new model for heat conduction of nanofluids based on fractal distributions of nanoparticles. *J. Phys. D Appl. Phys.* **2008**, *41*, 139801. [CrossRef]
31. Anoop, K.B.; Sundararajan, T.; Das, S.K. Effect of particle size on the convective heat transfer in nanofluid in the developing region. *Int. J. Heat Mass Transf.* **2009**, *52*, 2189–2195. [CrossRef]
32. Pil Jang, S.; Choi, S.U.S. Effects of Various Parameters on Nanofluid Thermal Conductivity. *J. Heat Transfer* **2006**, *129*, 617–623. [CrossRef]
33. Timofeeva, E.; Smith, D.; Yu, W.; France, D.; Singh, D.; Routbort, J. Particle size and interfacial effects on thermo-physical and heat transfer characteristics of water-basedalpha-SiC nanofluids. *Nanotechnology* **2010**, *21*, 215703. [CrossRef] [PubMed]
34. Murshed, S.M.S.; Leong, K.C.; Yang, C. Enhanced thermal conductivity of TiO2—Water based nanofluids. *Int. J. Therm. Sci.* **2005**, *44*, 367–373. [CrossRef]
35. Jeong, J.; Li, C.; Kwon, Y.; Lee, J.; Kim, S.H.; Yun, R. Particle shape effect on the viscosity and thermal conductivity of ZnO nanofluids. *Int. J. Refrig.* **2013**, *36*, 2233–2241. [CrossRef]
36. Timofeeva, E.V.; Routbort, J.L.; Singh, D. Particle shape effects on thermophysical properties of alumina nanofluids. *J. Appl. Phys.* **2009**, *106*, 14304. [CrossRef]
37. Glory, J.; Bonetti, M.; Helezen, M.; Mayne-L'Hermite, M.; Reynaud, C. Thermal and electrical conductivities of water-based nanofluids prepared with long multiwalled carbon nanotubes. *J. Appl. Phys.* **2008**, *103*, 94309. [CrossRef]
38. Gowda, R.; Sun, H.; Wang, P.; Charmchi, M.; Gao, F.; Gu, Z.; Budhlall, B. Effects of Particle Surface Charge, Species, Concentration, and Dispersion Method on the Thermal Conductivity of Nanofluids. *Adv. Mech. Eng.* **2010**, *2*, 807610. [CrossRef]
39. Chen, L.; Xie, H.; Li, Y.; Yu, W. Nanofluids containing carbon nanotubes treated by mechanochemical reaction. *Thermochim. Acta* **2008**, *477*, 21–24. [CrossRef]
40. Hwang, Y.-J.J.; Ahn, Y.C.; Shin, H.S.; Lee, C.G.; Kim, G.T.; Park, H.S.; Lee, J.K. Investigation on characteristics of thermal conductivity enhancement of nanofluids. *Curr. Appl. Phys.* **2006**, *6*, 1068–1071. [CrossRef]
41. Esfe, M.H.; Esfandeh, S.; Afrand, M.; Rejvani, M.; Rostamian, S.H. Experimental evaluation, new correlation proposing and ANN modeling of thermal properties of EG based hybrid nanofluid containing ZnO-DWCNT nanoparticles for internal combustion engines applications. *Appl. Therm. Eng.* **2018**, *133*, 452–463. [CrossRef]
42. Hemmat Esfe, M.; Yan, W.-M.; Akbari, M.; Karimipour, A.; Hassani, M. Experimental study on thermal conductivity of DWCNT-ZnO/water-EG nanofluids. *Int. Commun. Heat Mass Transf.* **2015**, *68*, 248–251. [CrossRef]
43. Rostamian, S.H.; Biglari, M.; Saedodin, S.; Hemmat Esfe, M. An inspection of thermal conductivity of CuO-SWCNTs hybrid nanofluid versus temperature and concentration using experimental data, ANN modeling and new correlation. *J. Mol. Liq.* **2017**, *231*, 364–369. [CrossRef]
44. Xuan, Y.; Li, Q. Heat transfer enhancement of nanofluids. *Int. J. Heat Fluid Flow* **2000**, *21*, 58–64. [CrossRef]
45. Jana, S.; Salehi-Khojin, A.; Zhong, W.-H. Enhancement of fluid thermal conductivity by the addition of single and hybrid nano-additives. *Thermochim. Acta* **2007**, *462*, 45–55. [CrossRef]
46. Choi, S.U.S.; Li, S.; Eastman, J.A. Measuring thermal conductivity of fluids containing oxide nanoparticles. *J. Heat Transf.* **1999**, *121*, 280–289.
47. Hong, J.; Kim, D. Effects of aggregation on the thermal conductivity of alumina/water nanofluids. *Thermochim. Acta* **2012**, *542*, 28–32. [CrossRef]
48. Keblinski, P.; Eastman, J.A.; Cahill, D.G. Nanofluids for thermal transport. *Mater. Today* **2005**, *8*, 36–44. [CrossRef]
49. Li, Q.; Xuan, Y.; Wang, J. Experimental investigations on transport properties of magnetic fluids. *Exp. Therm. Fluid Sci.* **2005**, *30*, 109–116. [CrossRef]
50. Nasiri, A.; Shariaty-Niasar, M.; Rashidi, A.; Amrollahi, A.; Khodafarin, R. Effect of dispersion method on thermal conductivity and stability of nanofluid. *Exp. Therm. Fluid Sci.* **2011**, *35*, 717–723. [CrossRef]
51. Devendiran, D.K.; Amirtham, V.A. A review on preparation, characterization, properties and applications of nanofluids. *Renew. Sustain. Energy Rev.* **2016**, *60*, 21–40. [CrossRef]
52. Salari, S.; Jafari, S.M. Application of nanofluids for thermal processing of food products. *Trends Food Sci. Technol.* **2020**, *97*, 100–113. [CrossRef]
53. Chon, C.H.; Kihm, K.D.; Lee, S.P.; Choi, S.U.S. Empirical correlation finding the role of temperature and particle size for nanofluid (Al2O3) thermal conductivity enhancement. *Appl. Phys. Lett.* **2005**, *87*, 153107. [CrossRef]

54. Mintsa, H.A.; Roy, G.; Nguyen, C.T.; Doucet, D. New temperature dependent thermal conductivity data for water-based nanofluids. *Int. J. Therm. Sci.* **2009**, *48*, 363–371. [CrossRef]
55. Shalkevich, N.; Escher, W.; Bürgi, T.; Michel, B.; Si-Ahmed, L.; Poulikakos, D. On the Thermal Conductivity of Gold Nanoparticle Colloids. *Langmuir* **2010**, *26*, 663–670. [CrossRef] [PubMed]
56. Duangthongsuk, W.; Wongwises, S. Measurement of temperature-dependent thermal conductivity and viscosity of TiO2-water nanofluids. *Exp. Therm. Fluid Sci.* **2009**, *33*, 706–714. [CrossRef]
57. Krishnakumar, T.S.; Viswanath, S.P.; Varghese, S.M. Experimental studies on thermal and rheological properties of Al2O3–ethylene glycol nanofluid. *Int. J. Refrig.* **2018**, *89*, 122–130.
58. Li, X.F.; Zhu, D.S.; Wang, X.J.; Wang, N.; Gao, J.W.; Li, H. Thermal conductivity enhancement dependent pH and chemical surfactant for Cu-H2O nanofluids. *Thermochim. Acta* **2008**, *469*, 98–103. [CrossRef]
59. Wang, X.; Li, X.; Yang, S. Influence of pH and SDBS on the Stability and Thermal Conductivity of Nanofluids. *Energy Fuels* **2009**, *23*, 2684–2689. [CrossRef]
60. Xie, H.; Yu, W.; Li, Y.; Chen, L. Discussion on the thermal conductivity enhancement of nanofluids. *Nanoscale Res. Lett.* **2011**, *6*, 124. [CrossRef] [PubMed]
61. Wamkam, C.T.; Opoku, M.K.; Hong, H.; Smith, P. Effects of *ph* on heat transfer nanofluids containing ZrO_2 and TiO_2 nanoparticles. *J. Appl. Phys.* **2011**, *109*, 024305. [CrossRef]
62. Zhu, D.; Li, X.; Wang, N.; Wang, X.; Gao, J.; Li, H. Dispersion behavior and thermal conductivity characteristics of Al2O3–H2O nanofluids. *Curr. Appl. Phys.* **2009**, *9*, 131–139. [CrossRef]
63. Eastman, J.A.; Choi, S.U.S.; Li, S.; Yu, W.; Thompson, L.J. Anomalously increased effective thermal conductivities of ethylene glycol-based nanofluids containing copper nanoparticles. *Appl. Phys. Lett.* **2001**, *78*, 718–720. [CrossRef]
64. Younes, H.; Christensen, G.; Luan, X.; Hong, H.; Smith, P. Effects of alignment, *ph*, surfactant, on heat transfer nanofluids containing Fe_2O_3 and CuO nanoparticles. *J. Appl. Phys.* **2012**, *111*, 064308. [CrossRef]
65. Hong, T.-K.K.; Yang, H.-S.S.; Choi, C.J. Study of the enhanced thermal conductivity of Fe nanofluids. *J. Appl. Phys.* **2005**, *97*, 64311. [CrossRef]
66. Garg, P.; Alvarado, J.L.; Marsh, C.; Carlson, T.A.; Kessler, D.A.; Annamalai, K. An experimental study on the effect of ultrasonication on viscosity and heat transfer performance of multi-wall carbon nanotube-based aqueous nanofluids. *Int. J. Heat Mass Transf.* **2009**, *52*, 5090–5101. [CrossRef]
67. Asadi, A.; Asadi, M.; Siahmargoi, M.; Asadi, T.; Gholami Andarati, M. The effect of surfactant and sonication time on the stability and thermal conductivity of water-based nanofluid containing Mg(OH)2 nanoparticles: An experimental investigation. *Int. J. Heat Mass Transf.* **2017**, *108*, 191–198. [CrossRef]
68. Hong, H.; Wright, B.; Wensel, J.; Jin, S.; Ye, X.R.; Roy, W. Enhanced thermal conductivity by the magnetic field in heat transfer nanofluids containing carbon nanotube. *Synthetic Metals* **2007**, *157*, 437–440. [CrossRef]
69. Wright, B.; Thomas, D.; Hong, H.; Groven, L.; Puszynski, J.; Duke, E.; Ye, X.; Jin, S. Magnetic field enhanced thermal conductivity in heat transfer nanofluids Ni coated single wall carbon nanotubes. *Appl. Phys. Lett.* **2007**, *91*, 173116. [CrossRef]
70. Wensel, J.; Wright, B.; Thomas, D.; Douglas, W.; Mannhalter, B.; Cross, W.; Hong, H.; Kellar, J.; Smith, P.; Roy, W. Enhanced thermal conductivity by aggregation in heat transfer nanofluids containing metal oxide nanoparticles and carbon nanotubes. *Appl. Phys. Lett.* **2008**, *92*, 023110. [CrossRef]
71. Das, P.K. A review based on the effect and mechanism of thermal conductivity of normal nanofluids and hybrid nanofluids. *J. Mol. Liq.* **2017**, *240*, 420–446. [CrossRef]
72. Lamas, B.; Abreu, B.; Fonseca, A.; Martins, N.; Oliveira, M. Critical analysis of the thermal conductivity models for CNT based nanofluids. *Int. J. Therm. Sci.* **2014**, *78*, 65–76. [CrossRef]
73. Maxwell, J.C. *A Treatise on Electricity and Magnetism*; Cambridge University Press: Cambridge, UK, 1873, ISBN 9780511709340.
74. Wasp, E.J.; Kenny, J.P.; Gandhi, R.L. Solid-liquid flow: Slurry pipeline transportation. Pumps, valves, mechanical equipment, economics. *Ser. Bulk Mater.Handl.* **1977**, *1*, 106804135.
75. Xuan, Y.; Li, Q.; Hu, W. Aggregation structure and thermal conductivity of nanofluids. *AIChE J.* **2003**, *49*, 1038–1043. [CrossRef]
76. Koo, J.; Kleinstreuer, C. A new thermal conductivity model for nanofluids. *J. Nanoparticle Res.* **2004**, *6*, 577–588. [CrossRef]
77. Xie, H.; Fujii, M.; Zhang, X. Effect of interfacial nanolayer on the effective thermal conductivity of nanoparticle-fluid mixture. *Int. J. Heat Mass Transf.* **2005**, *48*, 2926–2932. [CrossRef]
78. Avsec, J.; Oblak, M. The calculation of thermal conductivity, viscosity and thermodynamic properties for nanofluids on the basis of statistical nanomechanics. *Int. J. Mass Transf.* **2007**, *50*, 4331–4341. [CrossRef]
79. Pak, B.C.; Cho, Y.I. Hydrodynamic and heat transfer study of dispersed fluids with submicron metallic oxide particles. *Exp. Heat Transf.* **1998**, *11*, 151–170. [CrossRef]
80. Yu, W.; Choi, S.U.S. The role of interfacial layers in the enhanced thermal conductivity of nanofluids: A renovated Maxwell model. *J. Nanopart Res.* **2003**, *5*, 167–171. [CrossRef]
81. Wang, W.; Lin, L.; Zhou, X.; Wang, S. A Comprehensive Model for the Enhanced Thermal Conductivity of Nanofluids. *J. Adv. Res. Phys.* **2012**, *3*, 1–5.
82. Chandrasekar, M.; Suresh, S.; Srinivasan, R.; Bose, A.C. New Analytical Models to Investigate Thermal Conductivity of Nanofluids. *J. Nanosci. Nanotechnol.* **2009**, *9*, 533–538. [CrossRef] [PubMed]

83. Corcione, M. Empirical correlating equations for predicting the effective thermal conductivity and dynamic viscosity of nanofluids. *Energy Convers Manag.* **2011**, *52*, 789–793. [CrossRef]
84. Rocha, C.D.S. Study of the Cooling in Heat Sinks with the Recourse to Innovative Nanofluids. Master's Thesis, Department of Mechanical Engineering, Universidade do Minho, Braga, Portugal, 2018.
85. Zhang, Y.; Xu, X. Predicting the thermal conductivity enhancement of nanofluids using computacional intelligence. *Phys. Lett. A* **2020**, *384*, 126500. [CrossRef]
86. Sahaluddin, M.; Alade, I.O.; Oyedeji, M.O.; Aliyu, U.S. A machine learnig-based model to estimate the density of nanofluids of nitrides in ethylene glycol. *J. Appl. Phys.* **2020**, *127*, 205105. [CrossRef]
87. Alade, I.O.; Rahman, M.A.A.; Hassan, A.; Saleh, T.A. Modeling the viscosity of nanofluids using artificial neural network and Bayesan support vector regression. *J. Appl. Phys.* **2020**, *128*, 085306. [CrossRef]
88. Shateri, M.; Sobhanigavgani, Z.; Alinasab, A.; Varamesh, A.; Hemmati-Sarapardeh, A.; Mosavi, A.; Shahab, S. Comparative Analysis of Machine Learning Models for Nanofluids Viscosity Assessment. *Nanomaterials* **2020**, *10*, 1767. [CrossRef]
89. Zhang, Y.; Xu, X. Machine learning glass transition temperature of polyacrylamides using quantum chemical descriptors. *Polym. Chem.* **2021**, *12*, 843–851. [CrossRef]
90. Zhang, Y.; Xu, X. Machine learning glass transition temperature of polymers. *Heliyon* **2020**, *6*, e05055. [CrossRef]
91. Zhang, Y.; Xu, X. Machine Learning Decomposition Onset Temperature of Lubricant Additives. *J. Mater. Eng. Perform.* **2020**, *29*, 6605. [CrossRef]
92. Ma, T.; Guo, Z.; Lin, M.; Wang, Q. Recent trends on nanofluid heat transfer machine learning research applied to renewable energy. *Renew. Sustain. Energy Rev.* **2021**, *138*, 110494. [CrossRef]
93. Zhao, N.B.; Li, S.Y.; Yang, J.L. A review on nanofluids: Data-driven modeling of thermalphysical properties and the application in automotive radiator. *Renew. Sustain. Energy Rev.* **2016**, *66*, 596–616. [CrossRef]
94. Ramezanizadeh, M.; Ahmadi, M.H.; Nazari, M.A.; Sadeghzadeh, M.; Chen, L.G. A review on the utilized machine learning approaches for modeling the dynamic viscosity of nanofluids. *Renew. Sustain. Energy Rev.* **2019**, *114*, 109345. [CrossRef]
95. Bahiraei, M.; Heshmatian, S.; Moayedi, H. Artificial intelligence in the field of nanofluids: A review on applications and potencial future directions. *Powder Technol.* **2019**, *353*, 276–301. [CrossRef]
96. Guo, Z. A review on heat transfer enhancement with nanofluids. *J. Enhanc. Heat Transf.* **2020**, *27*, 1–70. [CrossRef]
97. Pavlik, M. The Dependence of Suspension Viscosity on Particle Size, Shear Rate, and Solvent Viscosity. Ph.D. Thesis, DePaul University, Chicago, IL, USA, 2009.
98. Brinkman, H.C. The viscosity of concentrated suspensions and solutions. *J. Chem. Phys.* **1952**, *20*, 571. [CrossRef]
99. Mooney, M. The viscosity of a concentrated suspension of spherical particles. *J. Colloid Sci.* **1951**, *6*, 162–170. [CrossRef]
100. Vajjha, R.S.; Das, D.K. Specific Heat Measurement of Three Nanofluids and Development of New Correlations. *J. Heat Transf.* **2009**, *131*, 071601. [CrossRef]
101. Nieh, H.-M.; Teng, T.-P.; Yu, C.-C. Enhanced heat dissipation of a radiator using oxide nano-coolant. *Int. J. Therm. Sci.* **2014**, *77*, 252–261. [CrossRef]
102. Lee, J.; Mudawar, I. Assessment of the effectiveness of nanofluids for single-phase and two-phase heat transfer in micro-channels. *Int. J. Heat Mass Transf.* **2007**, *50*, 452–463. [CrossRef]
103. Bergman, T.L. Effect of reduced specific heats of nanofluids on single phase, laminar internal forced convection. *Int. J. Heat Mass Transf.* **2009**, *52*, 1240–1244. [CrossRef]
104. Ho, C.J.; Wei, L.C.; Li, Z.W. An experimental investigation of forced convective cooling performance of a microchannel heat sink with Al2O3/water nanofluid. *Appl. Therm. Eng.* **2010**, *30*, 96–103. [CrossRef]
105. Al-Waeli, A.H.A.; Chaichan, M.T.; Kazem, H.A.; Sopian, K. Comparative study to use nano-(Al2O3, CuO, and SiC) with water to enhance photovoltaic thermal PV/T collectors. *Energy Convers. Manag.* **2017**, *148*, 963–973. [CrossRef]
106. Roberts, N.A.; Walker, D.G. Convective performance of nanofluids in commercial electronics cooling systems. *Appl. Therm. Eng.* **2010**, *30*, 2499–2504. [CrossRef]
107. Khaleduzzaman, S.S.; Sohel, M.R.; Saidur, R.; Mahbubul, I.M.; Shahrul, I.M.; Akash, B.A.; Selvaraj, J. Energy and exergy analysis of alumina-water nanofluid for an electronic liquid cooling system. *Int. Commun. Heat Mass Transf.* **2014**, *57*, 118–127. [CrossRef]
108. Li, C.H.; Peterson, G.P. Experimental investigation of temperature and volume fraction variations on the effective thermal conductivity of nanoparticle suspensions (nanofluids). *J. Appl. Phys.* **2006**, *99*, 084314. [CrossRef]
109. Li, C.H.; Peterson, G.P. The effect of particle size on the effective thermal conductivity of Al2O3-water nanofluids. *J. Appl. Phys.* **2007**, *101*, 44312. [CrossRef]
110. Zhang, X.; Gu, H.; Fujii, M. Effective thermal conductivity and thermal diffusivity of nanofluids containing spherical and cylindrical nanoparticles. *Exp. Therm. Fluid Sci.* **2007**, *31*, 593–599. [CrossRef]
111. Beck, M.P.; Yuan, Y.; Warrier, P.; Teja, A.S. The effect of particle size on the thermal conductivity of alumina nanofluids. *J. Nanoparticle Res.* **2009**, *11*, 1129–1136. [CrossRef]
112. Buonomo, B.; Manca, O.; Marinelli, L.; Nardini, S. Effect of temperature and sonication time on nanofluid thermal conductivity measurements by nano-flash method. *Appl. Therm. Eng.* **2015**, *91*, 181–190. [CrossRef]
113. Chandrasekar, M.; Suresh, S.; Chandra Bose, A. Experimental investigations and theoretical determination of thermal conductivity and viscosity of Al2O3/water nanofluid. *Exp. Therm. Fluid Sci.* **2010**, *34*, 210–216. [CrossRef]

114. Kim, S.H.; Choi, S.R.; Kim, D. Thermal Conductivity of Metal-Oxide Nanofluids: Particle Size Dependence and Effect of Laser Irradiation. *J. Heat Transf.* **2006**, *129*, 298–307. [CrossRef]
115. Kumar, N.; Sonawane, S.S.; Sonawane, S.H. Experimental study of thermal conductivity, heat transfer and friction factor of Al2O3 based nanofluid. *Int. Commun. Heat Mass Transf.* **2018**, *90*, 1–10. [CrossRef]
116. Beck, M.P.; Yuan, Y.; Warrier, P.; Teja, A.S. The thermal conductivity of alumina nanofluids in water, ethylene glycol, and ethylene glycol + water mixtures. *J. Nanoparticle Res.* **2010**, *12*, 1469–1477. [CrossRef]
117. Oh, D.-W.W.; Jain, A.; Eaton, J.K.; Goodson, K.E.; Lee, J.S. Thermal conductivity measurement and sedimentation detection of aluminum oxide nanofluids by using the 3ω method. *Int. J. Heat Fluid Flow* **2008**, *29*, 1456–1461. [CrossRef]
118. Usri, N.A.; Azmi, W.H.; Mamat, R.; Hamid, K.A.; Najafi, G. *Thermal Conductivity Enhancement of Al2O3 Nanofluid in Ethylene Glycol and Water Mixture*; Elsevier: Amsterdam, The Netherlands, 2015; Volume 79.
119. Khaleduzzaman, S.S.; Mahbubul, I.M.; Sohel, M.R.; Saidur, R.; Selvaraj, J.; Ward, T.A.; Niza, M.E. Experimental analysis of energy and friction factor for titanium dioxide nanofluid in a water block heat sink. *Int. J. Heat Mass Transf.* **2017**, *115*, 77–85. [CrossRef]
120. Narendran, G.; Bhat, M.M.; Akshay, L.; Arumuga Perumal, D. Experimental analysis on exergy studies of flow through a minichannel using Tio2/Water nanofluids. *Therm. Sci. Eng. Prog.* **2018**, *8*, 93–104. [CrossRef]
121. Zhang, J.; Diao, Y.; Zhao, Y.; Zhang, Y. Experimental study of TiO_2-water nanofluid flow and heat transfer characteristics in a multiport minichannel flat tube. *Int. J. Heat Mass Transf.* **2014**, *79*, 628–638. [CrossRef]
122. Xia, G.D.; Liu, R.; Wang, J.; Du, M. The characteristics of convective heat transfer in microchannel heat sinks using Al2O3 and TiO2 nanofluids. *Int. Commun. Heat Mass Transf.* **2016**, *76*, 256–264. [CrossRef]
123. Gan, Y.Y.; Ong, H.C.; Ling, T.C.; Zulkifli, N.W.M.; Wang, C.T.; Yang, Y.C. Thermal conductivity optimization and entropy generation analysis of titanium dioxide nanofluid in evacuated tube solar collector. *Appl. Therm. Eng.* **2018**, *145*, 155–164. [CrossRef]
124. He, Y.; Jin, Y.; Chen, H.; Ding, Y.; Cang, D.; Lu, H. Heat transfer and flow behavior of aqueous suspensions of TiO2 nanoparticles (nanofluids) flowing upward through a vertical pipe. *Int. J. Heat Mass Transf.* **2007**, *50*, 2272–2281. [CrossRef]
125. Krishnakumar, T.S.; Sheeba, A.; Mahesh, V.; Jose Prakash, M. Heat transfer studies on ethylene glycol/water nanofluid containing TiO2 nanoparticles. *Int. J. Refrig.* **2019**, *102*, 55–61. [CrossRef]
126. Khedkar, R.S.; Shrivastava, N.; Sonawane, S.S.; Wasewar, K.L. Experimental investigations and theoretical determination of thermal conductivity and viscosity of TiO2–ethylene glycol nanofluid. *Int. Commun. Heat Mass Transf.* **2016**, *73*, 54–61. [CrossRef]
127. Murshed, S.M.S.; Leong, K.C.; Yang, C. Investigations of thermal conductivity and viscosity of nanofluids. *Int. J. Therm. Sci.* **2008**, *47*, 560–568. [CrossRef]
128. Turgut, A.; Tavman, I.; Chirtoc, M.; Schuchmann, H.P.; Sauter, C.; Tavman, S. Thermal Conductivity and Viscosity Measurements of Water-Based TiO2 Nanofluids. *Int. J. Thermophys.* **2009**, *30*, 1213–1226. [CrossRef]
129. Al-Waeli, A.H.A.; Sopian, K.; Chaichan, M.T.; Kazem, H.A.; Hasan, H.A.; Al-Shamani, A.N. An experimental investigation of SiC nanofluid as a base-fluid for a photovoltaic thermal PV/T system. *Energy Convers. Manag.* **2017**, *142*, 547–558. [CrossRef]
130. Khedkar, R.S.; Sonawane, S.S.; Wasewar, K.L. Influence of CuO nanoparticles in enhancing the thermal conductivity of water and monoethylene glycol based nanofluids. *Int. Commun. Heat Mass Transf.* **2012**, *39*, 665–669. [CrossRef]
131. Agarwal, R.; Verma, K.; Agrawal, N.K.; Duchaniya, R.K.; Singh, R. Synthesis, characterization, thermal conductivity and sensitivity of CuO nanofluids. *Appl. Therm. Eng.* **2016**, *102*, 1024–1036. [CrossRef]
132. Hwang, Y.; Lee, J.K.; Lee, C.H.; Jung, Y.M.; Cheong, S.I.; Lee, C.G.; Ku, B.C.; Jang, S.P. Stability and thermal conductivity characteristics of nanofluids. *Thermochim. Acta* **2007**, *455*, 70–74. [CrossRef]
133. Naik, B.A.K.; Vinod, A.V. Heat transfer enhancement using non-Newtonian nanofluids in a shell and helical coil heat exchanger. *Exp. Therm. Fluid Sci.* **2018**, *90*, 132–142. [CrossRef]
134. Keyvani, M.; Afrand, M.; Toghraie, D.; Reiszadeh, M. An experimental study on the thermal conductivity of cerium oxide/ethylene glycol nanofluid: Developing a new correlation. *J. Mol. Liq.* **2018**, *266*, 211–217. [CrossRef]
135. Li, H.; Wang, L.; He, Y.; Hu, Y.; Zhu, J.; Jiang, B. Experimental investigation of thermal conductivity and viscosity of ethylene glycol based ZnO nanofluids. *Appl. Therm. Eng.* **2015**, *88*, 363–368. [CrossRef]
136. Yu, W.; Xie, H.; Chen, L.; Li, Y. Enhancement of thermal conductivity of kerosene-based Fe3O4 nanofluids prepared via phase-transfer method. *Colloids Surf. A Physicochem. Eng. Asp.* **2010**, *355*, 109–113. [CrossRef]
137. Abareshi, M.; Goharshadi, E.K.; Mojtaba Zebarjad, S.; Khandan Fadafan, H.; Youssefi, A. Fabrication, characterization and measurement of thermal conductivity of Fe3O4 nanofluids. *J. Magn. Magn. Mater.* **2010**, *322*, 3895–3901. [CrossRef]
138. Doganay, S.; Turgut, A.; Cetin, L. Magnetic field dependent thermal conductivity measurements of magnetic nanofluids by 3ω method. *J. Magn. Magn. Mater.* **2019**, *474*, 199–206. [CrossRef]
139. Karimi, A.; Sadatlu, M.A.A.; Saberi, B.; Shariatmadar, H.; Ashjaee, M. Experimental investigation on thermal conductivity of water based nickel ferrite nanofluids. *Adv. Powder Technol.* **2015**, *26*, 1529–1536. [CrossRef]
140. Hemmat Esfe, M.; Afrand, M.; Karimipour, A.; Yan, W.-M.; Sina, N. An experimental study on thermal conductivity of MgO nanoparticles suspended in a binary mixture of water and ethylene glycol. *Int. Commun. Heat Mass Transf.* **2015**, *67*, 173–175. [CrossRef]
141. Liu, M.-S.; Lin, M.C.-C.; Tsai, C.Y.; Wang, C.-C. Enhancement of thermal conductivity with Cu for nanofluids using chemical reduction method. *Int. J. Heat Mass Transf.* **2006**, *49*, 3028–3033. [CrossRef]

142. Putnam, S.A.; Cahill, D.G.; Braun, P.V.; Ge, Z.; Shimmin, R.G. Thermal conductivity of nanoparticle suspensions. *J. Appl. Phys.* **2006**, *99*, 84308. [CrossRef]
143. Carbajal-Valdéz, R.; Rodríguez-Juárez, A.; Jiménez-Pérez, J.L.; Sánchez-Ramírez, J.F.; Cruz-Orea, A.; Correa-Pacheco, Z.N.; Macias, M.; Luna-Sánchez, J.L. Experimental investigation on thermal properties of Ag nanowire nanofluids at low concentrations. *Thermochim. Acta* **2019**, *671*, 83–88. [CrossRef]
144. Parametthanuwat, T.; Bhuwakietkumjohn, N.; Rittidech, S.; Ding, Y. Experimental investigation on thermal properties of silver nanofluids. *Int. J. Heat Fluid Flow* **2015**, *56*, 80–90. [CrossRef]
145. Alirezaie, A.; Hajmohammad, M.H.; Hassani Ahangar, M.R.; Hemmat Esfe, M. Price-performance evaluation of thermal conductivity enhancement of nanofluids with different particle sizes. *Appl. Therm. Eng.* **2018**, *128*, 373–380. [CrossRef]
146. Lee, S.W.; Park, S.D.; Kang, S.; Bang, I.C.; Kim, J.H. Investigation of viscosity and thermal conductivity of SiC nanofluids for heat transfer applications. *Int. J. Heat Mass Transf.* **2011**, *54*, 433–438. [CrossRef]
147. Li, X.; Zou, C.; Zhou, L.; Qi, A. Experimental study on the thermo-physical properties of diathermic oil based SiC nanofluids for high temperature applications. *Int. J. Heat Mass Transf.* **2016**, *97*, 631–637. [CrossRef]
148. Ranjbarzadeh, R.; Moradikazerouni, A.; Bakhtiari, R.; Asadi, A.; Afrand, M. An experimental study on stability and thermal conductivity of water/silica nanofluid: Eco-friendly production of nanoparticles. *J. Clean. Prod.* **2019**, *206*, 1089–1100. [CrossRef]
149. Mousavi, S.M.; Esmaeilzadeh, F.; Wang, X.P. A detailed investigation on the thermo-physical and rheological behavior of MgO/TiO2 aqueous dual hybrid nanofluid. *J. Mol. Liq.* **2019**, *282*, 323–339. [CrossRef]
150. Sarafraz, M.M.; Yang, B.; Pourmehran, O.; Arjomandi, M.; Ghomashchi, R. Fluid and heat transfer characteristics of aqueous graphene nanoplatelet (GNP) nanofluid in a microchannel. *Int. Commun. Heat Mass Transf.* **2019**, *107*, 24–33. [CrossRef]
151. Yu, W.; Xie, H.; Wang, X.; Wang, X. Significant thermal conductivity enhancement for nanofluids containing graphene nanosheets. *Phys. Lett. A* **2011**, *375*, 1323–1328. [CrossRef]
152. Arzani, H.K.; Amiri, A.; Kazi, S.N.; Chew, B.T.; Badarudin, A. Experimental and numerical investigation of thermophysical properties, heat transfer and pressure drop of covalent and noncovalent functionalized graphene nanoplatelet-based water nanofluids in an annular heat exchanger. *Int. Commun. Heat Mass Transf.* **2015**, *68*, 267–275. [CrossRef]
153. Bhattad, A.; Sarkar, J.; Ghosh, P. Experimentation on effect of particle ratio on hydrothermal performance of plate heat exchanger using hybrid nanofluid. *Appl. Therm. Eng.* **2019**, *162*, 114309. [CrossRef]
154. Poongavanam, G.K.; Panchabikesan, K.; Murugesan, R.; Duraisamy, S.; Ramalingam, V. Experimental investigation on heat transfer and pressure drop of MWCNT—Solar glycol based nanofluids in shot peened double pipe heat exchanger. *Powder Technol.* **2019**, *345*, 815–824. [CrossRef]
155. Rehman, W.U.; Merican, Z.M.A.; Bhat, A.H.; Hoe, B.G.; Sulaimon, A.A.; Akbarzadeh, O.; Khan, M.S.; Mukhtar, A.; Saqib, S.; Hameed, A.; et al. Synthesis, characterization, stability and thermal conductivity of multi-walled carbon nanotubes (MWCNTs) and eco-friendly jatropha seed oil based nanofluid: An experimental investigation and modeling approach. *J. Mol. Liq.* **2019**, *293*, 111534. [CrossRef]
156. Ding, Y.; Alias, H.; Wen, D.; Williams, R.A. Heat transfer of aqueous suspensions of carbon nanotubes (CNT nanofluids). *Int. J. Heat Mass Transf.* **2006**, *49*, 240–250. [CrossRef]
157. Assael, M.J.; Metaxa, I.N.; Arvanitidis, J.; Christofilos, D.; Lioutas, C. Thermal Conductivity Enhancement in Aqueous Suspensions of Carbon Multi-Walled and Double-Walled Nanotubes in the Presence of Two Different Dispersants. *Int. J. Thermophys.* **2005**, *26*, 647–664. [CrossRef]
158. Xing, M.; Yu, J.; Wang, R. Experimental investigation and modeling on the thermal conductivity of CNTs based nanofluids. *Int. J. Therm. Sci.* **2016**, *104*, 404–411. [CrossRef]
159. Fakoor Pakdaman, M.; Akhavan-Behabadi, M.A.; Razi, P. An experimental investigation on thermo-physical properties and overall performance of MWCNT/heat transfer oil nanofluid flow inside vertical helically coiled tubes. *Exp. Therm. Fluid Sci.* **2012**, *40*, 103–111. [CrossRef]
160. Liu, M.-S.; Ching-Cheng Lin, M.; Huang, I.-T.; Wang, C.-C. Enhancement of thermal conductivity with carbon nanotube for nanofluids. *Int. Commun. Heat Mass Transf.* **2005**, *32*, 1202–1210. [CrossRef]
161. Harish, S.; Ishikawa, K.; Einarsson, E.; Aikawa, S.; Chiashi, S.; Shiomi, J.; Maruyama, S. Enhanced thermal conductivity of ethylene glycol with single-walled carbon nanotube inclusions. *Int. J. Heat Mass Transf.* **2012**, *55*, 3885–3890. [CrossRef]